

UC Berkeley
SEMM Reports Series

Title

A Quadrilateral Mixed Finite Element With Two Enhanced Strain Modes

Permalink

<https://escholarship.org/uc/item/3fr937dq>

Authors

Piltner, Reinhard
Taylor, Robert

Publication Date

1994-03-01

REPORT NO.
UCB/SEMM-94/05

**STRUCTURAL ENGINEERING,
MECHANICS AND MATERIALS**

**A QUADRILATERAL MIXED FINITE ELEMENT
WITH TWO ENHANCED STRAIN MODES**

BY

R. PILTNER and R.L. TAYLOR

MARCH 1994

**DEPARTMENT OF CIVIL ENGINEERING
UNIVERSITY OF CALIFORNIA
BERKELEY, CALIFORNIA**

A QUADRILATERAL MIXED FINITE ELEMENT WITH TWO ENHANCED STRAIN MODES

R. PILTNER and R.L. TAYLOR

Department of Civil Engineering, SEMM, University of California at Berkeley,
Berkeley, CA 94720, U.S.A.

An improved plane strain/stress element is derived using a Hu-Washizu variational formulation with bilinear displacement interpolation, seven strain and stress terms, and two enhanced strain modes. The number of unknowns of the four-node element is increased from eight to ten degrees of freedom. For linear and nonlinear applications, the two unknowns associated with the enhanced strain terms can be eliminated by static condensation so that eight displacement degrees of freedom remain for the proposed element, which is denoted by QE2. The excellent performance of the proposed element is demonstrated using several linear and non-linear examples.

1. Introduction

The standard four node compatible displacement element shows poor performance for problems with bending and for plane strain problems in the nearly incompressible limit. Several methods have been developed to overcome these problems.

For the improvement of the performance of the four node element, Wilson et al. [1] proposed to use four incompatible displacement modes with quadratic variation. However, the resulting element did not pass the constant strain patch test.

In order to be able to pass the patch test, Taylor et al. [2] proposed a modification which resulted in a well performing element. Recently Simo and Rifai [3] introduced the method of "enhanced strains" and they found that the aforementioned Taylor/Beresford/Wilson element (denoted by QM6) can be viewed as an enhanced strain element with four enhanced strain terms. A discussion about the construction of suitable incompatible displacements which lead to convergent elements was given by Wu, Huang and Pian [4].

Hughes [5] used selected reduced integration to improve the performance of the four node element and introduced the so called B-bar method [6].

Using incompatible displacements, Pian and Sumihara [7] introduced a method to construct an assumed stress field in natural coordinates with a minimum number of terms. Their assumed hybrid stress element has only five parameters and is an excellent performer especially in tests for evaluating the element behavior under mesh distortion in bending applications.

The original five parameter hybrid stress element of Pian [8] was formulated in cartesian coordinates. Since the five parameter stress field is an incomplete linear stress field, the original Pian element is not frame invariant. Spilker et al. [9] used a seven parameter stress field which is a complete linear stress field in cartesian coordinates. However, the seven parameter element turned out to be too stiff.

The Pian/Sumihara element with five stress terms in natural coordinates is flexible because it has the minimum number of terms possible. Using ND as the number of unknowns of the element and NS as the number of stress terms we have the requirement

$$NS \geq ND - 3 \tag{1}$$

which means that the minimum number of stress terms is the number of element unknowns minus the number of rigid body terms. Using more terms than the minimum number makes an element too stiff. For the case of the Pian/Sumihara element, we achieve an optimal situation since $ND = 8$ and $NS = 5$. The Pian/Sumihara stress terms satisfy equilibrium in a weak sense.

If we use incompatible displacements in addition to the eight compatible displacements we can increase the number of stress terms. In this paper we will choose a complete linear set of seven stress and strain terms in cartesian coordinates. For the case of linear elastic materials the stress-strain relations and the equilibrium equations will be satisfied pointwise. Two additional strain terms are used in order to get a flexible element. After condensation of the additional two degrees of freedom, the element has eight degrees of freedom.

In several numerical examples, the proposed element is compared to the standard compatible displacement element (Q4) and to two of the best performing four-node elements, which are the Pian/Sumihara and the Taylor/Beresford/Wilson elements. The different

underlying concepts of the compared elements can be seen from the following brief characterization.

- (i) The standard four-node displacement element (Q4) uses compatible shape functions in natural element coordinates. The element has eight degrees of freedom.
- (ii) The Pian/Sumihara element is a hybrid stress element. Stresses are assumed in natural coordinates. The stresses satisfy the equilibrium equations in a weak (integral) sense. Five stress terms are used. The stress terms do not include the bilinear term $\xi\eta$. The element has eight degrees of freedom. No condensation of extra degrees of freedom is needed. The element is well suited for linear applications.
- (iii) The Taylor/Beresford/Wilson element is an enhanced strain element with four enhanced terms. The enhanced strains are assumed in natural coordinates. For a general quadrilateral element shape (non rectangular shape and not a parallelogram) the strain modes are not polynomials in natural coordinates, they are rational functions in general and do not satisfy the equilibrium equations. The 12x12 stiffness matrix is condensed to a 8x8 element matrix. The element is suited for linear and nonlinear applications.
- (iv) For the proposed element, the stresses and strains are constructed by using local cartesian coordinates. Seven terms are used for the stress and strain fields. For the linear elastic case the resulting stresses form a complete set of linear functions which satisfy the equilibrium equations pointwise. Written in natural coordinates stresses and strains are also polynomials in these coordinates. The strains/stresses include the bilinear term $\xi\eta$. A 10x10 element stiffness matrix is computed. Only two extra degrees of freedom have to be condensed to obtain the final 8x8 stiffness matrix. The element can be used for linear and nonlinear applications.

2. Variational formulation

For hybrid elements Pian and Tong [10] introduced the concept of using incompatible displacements in the variational formulation. The concept was further discussed in reference [11].

For our finite element approximation, we consider the following modified Hu-Washizu variational formulation:

$$\Pi(\tilde{\mathbf{u}}, \boldsymbol{\varepsilon}^i, \boldsymbol{\varepsilon}, \boldsymbol{\sigma}) = \int_{\bar{V}} W(\boldsymbol{\varepsilon}) dV - \int_{\bar{V}} \tilde{\mathbf{u}}^T \bar{\mathbf{f}} dV - \int_{\bar{S}} \tilde{\mathbf{u}}^T \bar{\mathbf{T}} dS - \int_{\bar{V}} \boldsymbol{\sigma}^T (\boldsymbol{\varepsilon} - \mathbf{D}\tilde{\mathbf{u}} - \boldsymbol{\varepsilon}^i) dV. \quad (2)$$

In the used notation $\bar{\mathbf{f}}$ is the vector of given body forces and $\bar{\mathbf{T}}$ are prescribed tractions on the boundary \bar{S} . In our finite element approximation, we will use a strain field $\boldsymbol{\varepsilon}$ which can be obtained from a displacement field through the relation

$$\boldsymbol{\varepsilon} = \mathbf{D}\mathbf{u} \quad (3)$$

where \mathbf{D} is a linear differential operator matrix. The variation of (2) with respect to the stresses gives us the equation

$$\int_{\bar{V}} \delta \boldsymbol{\sigma}^T [\boldsymbol{\varepsilon} - \mathbf{D}\tilde{\mathbf{u}} - \boldsymbol{\varepsilon}^i] dV = 0 \quad (4)$$

The strains $\boldsymbol{\varepsilon}^i$ can be viewed as an enhanced strain field which is added to the compatible strains ($\mathbf{D}\tilde{\mathbf{u}}$). Equation (4) enables us to make an assumed strain field $\boldsymbol{\varepsilon}$ close to the strains ($\mathbf{D}\tilde{\mathbf{u}} + \boldsymbol{\varepsilon}^i$). One possibility of constructing the enhanced strain field $\boldsymbol{\varepsilon}^i$ is to use an incompatible displacement field \mathbf{u}^i and to get $\boldsymbol{\varepsilon}^i$ from

$$\boldsymbol{\varepsilon}^i = \mathbf{D}\mathbf{u}^i \quad (5)$$

in this case we can rewrite (4) as

$$\int_{\bar{V}} \delta \boldsymbol{\sigma}^T [\boldsymbol{\varepsilon} - \mathbf{D}(\tilde{\mathbf{u}} + \mathbf{u}^i)] dV = 0 \quad (6)$$

If we use stresses $\boldsymbol{\sigma}$ which satisfy the homogeneous equilibrium equations

$$\mathbf{D}^T \boldsymbol{\sigma} = \mathbf{0} \quad (7)$$

we can rewrite equation (6) as a boundary integral. Using the relationship

$$\int_{\bar{V}} \boldsymbol{\sigma}^T (\mathbf{D}\mathbf{u}) dV = - \int_{\bar{V}} (\mathbf{D}^T \boldsymbol{\sigma}) \mathbf{u} dV + \int_{\bar{S}} \mathbf{T}^T \mathbf{u} dS \quad (8)$$

equation (6) becomes

$$\int_{\bar{S}} \delta \mathbf{T}^T [\mathbf{u} - (\tilde{\mathbf{u}} + \mathbf{u}^i)] dS = 0 \quad (9)$$

where the tractions \mathbf{T} are obtained from

$$\mathbf{T} = \mathbf{n}\boldsymbol{\sigma} \quad (10)$$

and \mathbf{n} is the matrix of direction cosines on the boundary. Equation (6) can be used to make a chosen field $\boldsymbol{\varepsilon}$ close to the strains $\mathbf{D}(\tilde{\mathbf{u}} + \mathbf{u}^i)$ in an integral sense. Equivalently,

equation (9) provides a way of making the displacements \mathbf{u} close to $(\tilde{\mathbf{u}} + \mathbf{u}^i)$. In the notation used, $\tilde{\mathbf{u}}$ is a compatible displacement field containing shape functions and nodal displacements \mathbf{q} . In addition to the compatible displacements $\tilde{\mathbf{u}}$ we use incompatible displacements $\mathbf{u}^i = \mathbf{U}^i \lambda$ on which we will impose some restrictions in order to get an admissible strain field $\boldsymbol{\varepsilon}^i = \mathbf{B}^i \lambda$. The field $\boldsymbol{\varepsilon}^i$ can also be constructed directly. A simple method for the construction of $\boldsymbol{\varepsilon}^i$ was proposed by Taylor/Beresford/Wilson [2] in 1976. Examples for the choice of $\boldsymbol{\varepsilon}^i$ will be considered in section 6.

If we choose $\boldsymbol{\varepsilon}^i = \mathbf{0}$ for the functional Π , we get the standard form of the Hu-Washizu variational formulation for compatible displacements $\tilde{\mathbf{u}}$.

Carrying out the variation in (1) we obtain

$$\begin{aligned}
 \delta \Pi = & \int_{\mathbf{V}} \delta \boldsymbol{\varepsilon}^T \left[\frac{\partial \mathbf{W}(\boldsymbol{\varepsilon})}{\partial \boldsymbol{\varepsilon}} - \boldsymbol{\sigma} \right] dV \\
 & - \int_{\mathbf{V}} \delta \boldsymbol{\sigma}^T \left[\boldsymbol{\varepsilon} - \mathbf{D} \tilde{\mathbf{u}} - \boldsymbol{\varepsilon}^i \right] dV \\
 & - \int_{\mathbf{V}} \delta \tilde{\mathbf{u}}^T \left[\mathbf{D} \boldsymbol{\sigma}^T + \bar{\mathbf{f}} \right] dV + \int_{\mathbf{S}} \delta \tilde{\mathbf{u}}^T \left[\mathbf{T} - \bar{\mathbf{T}} \right] dS \\
 & + \int_{\mathbf{V}} (\delta \boldsymbol{\varepsilon}^i)^T \boldsymbol{\sigma} dV = 0
 \end{aligned} \tag{11}$$

The purpose of using enhanced strains $\boldsymbol{\varepsilon}^i$ is to make an element more flexible and thus improve the overall performance of the element. In the choice for the enhanced strains $\boldsymbol{\varepsilon}^i$ we are not completely free: In order to satisfy the patch test we have to impose the restriction on $\boldsymbol{\varepsilon}^i$ that constant stresses $\boldsymbol{\sigma}_c$ do no work on the enhanced strains. This requirement can be expressed in the form

$$\int_{\mathbf{V}} \delta \boldsymbol{\sigma}_c^T \boldsymbol{\varepsilon}^i dV = 0 \tag{12}$$

or equivalently as

$$\int_{\mathbf{V}} \boldsymbol{\varepsilon}^i dV = \mathbf{0} \tag{13}$$

If we would require that the enhanced strains are orthogonal to all stress terms by satisfying

$$\int_{\mathbf{V}} \delta \boldsymbol{\sigma}^T \boldsymbol{\varepsilon}^i dV = 0 \tag{14}$$

a priori, we would not be able to calculate any parameters λ for the field ε^i . The orthogonality requirement (14) is too strong for the kind of approximation we have in mind. Instead of requiring equation (14) to be satisfied we construct an admissible strain field ε^i by enforcing orthogonality to reference stresses σ^* , which, for the four node element, consist of constant and linear terms in ξ, η . In this case we have to satisfy a priori the following equation:

$$\int_{\mathbf{v}} \delta \sigma^{*T} \varepsilon^i dV = \int_{\mathbf{v}} \delta \varepsilon^{iT} \sigma^* dV = 0 \quad (15)$$

A comparison of the version of the enhanced strain formulation considered in this paper to the version proposed by Simo and Rifai is made in the appendix.

3. Finite element approximations for the linear elastic case

In the case of linear elasticity the strain energy density function can be written in the form

$$W(\varepsilon) = \frac{1}{2} \varepsilon^T \mathbf{E} \varepsilon \quad (16)$$

so that for $\partial W(\varepsilon)/\partial \varepsilon$ we get

$$\sigma = \frac{\partial W(\varepsilon)}{\partial \varepsilon} = \mathbf{E} \varepsilon, \quad (17)$$

where

$$\mathbf{E} = \frac{\mathbf{E}}{(1+\nu)(1-2\nu)} \begin{bmatrix} 1-\nu & \nu & 0 \\ \nu & 1-\nu & 0 \\ 0 & 0 & (1-2\nu)/2 \end{bmatrix} \quad (18)$$

for plane strain, and

$$\mathbf{E} = \frac{\mathbf{E}}{1-\nu^2} \begin{bmatrix} 1 & \nu & 0 \\ \nu & 1 & 0 \\ 0 & 0 & (1-\nu)/2 \end{bmatrix} \quad (19)$$

for plane stress. The displacement, strain, and stress fields are chosen in the following form:

$$\tilde{\mathbf{u}} = \mathbf{N} \mathbf{q}$$

$$\boldsymbol{\varepsilon} = \mathbf{A}\boldsymbol{\beta} \quad (20)$$

$$\boldsymbol{\sigma} = \mathbf{E}\boldsymbol{\varepsilon} = \mathbf{E}\mathbf{A}\boldsymbol{\beta} = \mathbf{P}\boldsymbol{\beta}$$

$$\boldsymbol{\varepsilon}^i = \mathbf{B}^i\boldsymbol{\lambda}.$$

From the compatible displacement field $\tilde{\mathbf{u}}$ involving the matrix of shape functions \mathbf{N} and the nodal displacement \mathbf{q} we obtain the strains as

$$\tilde{\boldsymbol{\varepsilon}} = \mathbf{D}\tilde{\mathbf{u}} = \mathbf{D}\mathbf{N}\mathbf{q} = \mathbf{B}\mathbf{q} \quad (21)$$

where \mathbf{B} is the standard strain matrix for isoparametric finite elements. Using equation (3) the strain field $\boldsymbol{\varepsilon}$ is obtained from a displacement field

$$\mathbf{u} = \mathbf{U}\boldsymbol{\beta} \quad (22)$$

so that the strain matrix \mathbf{A} and the stress matrix \mathbf{P} are obtained from

$$\mathbf{A} = \mathbf{D}\mathbf{U} \quad (23)$$

$$\mathbf{P} = \mathbf{E}\mathbf{A} = \mathbf{E}\mathbf{D}\mathbf{U}. \quad (24)$$

For the displacement field \mathbf{u} we will construct linearly independent functions which a priori satisfy the Navier-equations

$$\mathbf{D}^T\mathbf{E}\mathbf{D}\mathbf{u} = \mathbf{0}. \quad (25)$$

Since the chosen functions for $\boldsymbol{\varepsilon}$ and $\boldsymbol{\sigma}$ are related to \mathbf{u} as indicated above we also satisfy the equations

$$\mathbf{D}^T\mathbf{E}\boldsymbol{\varepsilon} = \mathbf{0} \quad (26)$$

and

$$\mathbf{D}^T\boldsymbol{\sigma} = \mathbf{0}. \quad (27)$$

After substituting relationships (16) and (17) and the assumed fields (20) into (2) we obtain Π in the following form:

$$\Pi = -\frac{1}{2}\boldsymbol{\beta}^T\mathbf{H}\boldsymbol{\beta} + \boldsymbol{\beta}^T\mathbf{L}\mathbf{q} + \boldsymbol{\beta}^T\mathbf{L}^i\boldsymbol{\lambda} - \mathbf{q}^T\mathbf{f}_{\text{ext}} \quad (28)$$

where

$$\begin{aligned} \mathbf{H} &= \int_{\mathbf{v}} \mathbf{A}^T\mathbf{E}\mathbf{A} \, dV = \int_{\mathbf{v}} \mathbf{P}^T\mathbf{E}^{-1}\mathbf{P} \, dV \\ \mathbf{L} &= \int_{\mathbf{v}} \mathbf{A}^T\mathbf{E}\mathbf{B} \, dV = \int_{\mathbf{v}} \mathbf{P}^T\mathbf{B} \, dV \\ \mathbf{L}^i &= \int_{\mathbf{v}} \mathbf{A}^T\mathbf{E}\mathbf{B}^i \, dV = \int_{\mathbf{v}} \mathbf{P}^T\mathbf{B}^i \, dV \end{aligned} \quad (29)$$

$$\mathbf{f}_{\text{ext}} = \int_V \mathbf{N}^T \bar{\mathbf{f}} dV + \int_S \mathbf{N}^T \bar{\mathbf{T}} dS$$

The variation of Π with respect to $\boldsymbol{\beta}$, \mathbf{q} and $\boldsymbol{\lambda}$ gives us the following system of equations:

$$\begin{bmatrix} -\mathbf{H} & \mathbf{L} & \mathbf{L}^i \\ \mathbf{L}^T & \mathbf{0} & \mathbf{0} \\ \mathbf{L}^{iT} & \mathbf{0} & \mathbf{0} \end{bmatrix} \begin{bmatrix} \boldsymbol{\beta} \\ \mathbf{q} \\ \boldsymbol{\lambda} \end{bmatrix} = \begin{bmatrix} \mathbf{0} \\ \mathbf{f}_{\text{ext}} \\ \mathbf{0} \end{bmatrix} \quad (30)$$

The strain and stress parameters $\boldsymbol{\beta}$ can be expressed in terms of the nodal displacements \mathbf{q} and the enhanced strain parameters $\boldsymbol{\lambda}$ in the form

$$\boldsymbol{\beta} = \mathbf{H}^{-1} \mathbf{L} \mathbf{q} + \mathbf{H}^{-1} \mathbf{L}^i \boldsymbol{\lambda} \quad (31)$$

Using this relation we can reduce the system of equations (30) and get

$$\begin{bmatrix} \mathbf{K} & \boldsymbol{\Gamma}^T \\ \boldsymbol{\Gamma} & \mathbf{Q} \end{bmatrix} \begin{bmatrix} \mathbf{q} \\ \boldsymbol{\lambda} \end{bmatrix} = \begin{bmatrix} \mathbf{f}_{\text{ext}} \\ \mathbf{0} \end{bmatrix} \quad (32)$$

where

$$\begin{aligned} \mathbf{K} &= \mathbf{L}^T \mathbf{H}^{-1} \mathbf{L} \\ \boldsymbol{\Gamma} &= \mathbf{L}^i{}^T \mathbf{H}^{-1} \mathbf{L} \\ \mathbf{Q} &= \mathbf{L}^i{}^T \mathbf{H}^{-1} \mathbf{L}^i. \end{aligned} \quad (33)$$

Since the vector $\boldsymbol{\lambda}$ contains only internal element parameters which are not associated to any nodes we can apply a static condensation procedure to the system of equations (32) and obtain the reduced system

$$\mathbf{k} \mathbf{q} = \mathbf{f}_{\text{ext}} \quad (34)$$

where the element stiffness matrix is given by

$$\mathbf{k} = \mathbf{K} - \boldsymbol{\Gamma}^T \mathbf{Q}^{-1} \boldsymbol{\Gamma} \quad (35)$$

Once the nodal displacements \mathbf{q} are known for every element we get the vector of internal parameters from the equation

$$\boldsymbol{\lambda} = -\mathbf{Q}^{-1} \boldsymbol{\Gamma} \mathbf{q}. \quad (36)$$

For the linear elastic case, the stresses and strains in the element can be written in the form

$$\begin{aligned} \boldsymbol{\varepsilon}(\mathbf{x}) &= \mathbf{A}(\mathbf{x}) \left[\mathbf{H}^{-1} \mathbf{L} \mathbf{q} + \mathbf{H}^{-1} \mathbf{L}^i \boldsymbol{\lambda} \right] \\ \boldsymbol{\sigma}(\mathbf{x}) &= \mathbf{P}(\mathbf{x}) \left[\mathbf{H}^{-1} \mathbf{L} \mathbf{q} + \mathbf{H}^{-1} \mathbf{L}^i \boldsymbol{\lambda} \right] \end{aligned} \quad (37)$$

where λ is calculated from (36).

4. Finite element approximations for the case of non-linear materials

For a non-linear, hyperelastic material the stresses are obtained from a strain energy density function, $W(\boldsymbol{\varepsilon}^e)$, through

$$\tilde{\boldsymbol{\sigma}} = \frac{\partial W(\boldsymbol{\varepsilon}^e(\mathbf{x}))}{\partial \boldsymbol{\varepsilon}} \quad (38)$$

The stresses in this relationship are denoted by $\tilde{\boldsymbol{\sigma}}$ in order to distinguish them from the assumed finite element stresses $\boldsymbol{\sigma}$. If plastic deformations are present in the material the total strain $\boldsymbol{\varepsilon}$ will be decomposed into an elastic and a plastic part according to

$$\boldsymbol{\varepsilon} = \boldsymbol{\varepsilon}^e + \boldsymbol{\varepsilon}^p. \quad (39)$$

The strain energy density W in this case is expressed as a function of the elastic strain $\boldsymbol{\varepsilon}^e$ so that we assume W in the form

$$W = W(\boldsymbol{\varepsilon} - \boldsymbol{\varepsilon}^p). \quad (40)$$

The non-linear constitutive equations lead to a non-linear boundary value problem in which the load will be increased in increments from time t_n to time t_{n+1} . For time t_n we assume the physical quantities $\tilde{\mathbf{u}}_n$, $\boldsymbol{\varepsilon}_n$ and $\boldsymbol{\sigma}_n$ as given. For an increment in the load we seek the increments of displacements, strains and stresses. At $t = t_{n+1}$ we have

$$\begin{aligned} \tilde{\mathbf{u}}_{n+1} &= \tilde{\mathbf{u}}_n + \Delta \tilde{\mathbf{u}} \\ \boldsymbol{\varepsilon}_{n+1} &= \boldsymbol{\varepsilon}_n + \Delta \boldsymbol{\varepsilon} \\ \boldsymbol{\varepsilon}_{n+1}^i &= \boldsymbol{\varepsilon}_n^i + \Delta \boldsymbol{\varepsilon}^i \\ \boldsymbol{\sigma}_{n+1} &= \boldsymbol{\sigma}_n + \Delta \boldsymbol{\sigma} \\ \left[\frac{\partial W}{\partial \boldsymbol{\varepsilon}} \right]_{n+1} &= \left[\frac{\partial W}{\partial \boldsymbol{\varepsilon}} \right]_n + \Delta \left[\frac{\partial W}{\partial \boldsymbol{\varepsilon}} \right] = \boldsymbol{\sigma}_n + \Delta \tilde{\boldsymbol{\sigma}} \end{aligned} \quad (41)$$

and

$$\begin{aligned} \bar{\mathbf{T}}_{n+1} &= \bar{\mathbf{T}}_n + \Delta \bar{\mathbf{T}} \\ \bar{\mathbf{f}}_{n+1} &= \bar{\mathbf{f}}_n + \Delta \bar{\mathbf{f}} \end{aligned} \quad (42)$$

Our unknowns are the increments $\Delta \tilde{\mathbf{u}}$, $\Delta \boldsymbol{\varepsilon}$, $\Delta \boldsymbol{\varepsilon}^i$, $\Delta \boldsymbol{\sigma}$, $\Delta \tilde{\boldsymbol{\sigma}}$, whereas the load increments $\Delta \bar{\mathbf{T}}$ and $\Delta \bar{\mathbf{f}}$ are given (chosen) quantities.

Since our problem is non-linear, it is in general not possible to obtain, for an increment of the external load, the increments $\Delta\tilde{\mathbf{u}}$, $\Delta\varepsilon$, $\Delta\varepsilon^i$, $\Delta\sigma$ in one step. In order to solve the set of non-linear equations it becomes necessary to iterate. Denoting the final vector of global unknowns (displacements) with \mathbf{q} , the nonlinear system of equations can be written in the form

$$\mathbf{F}(\mathbf{q}) - \mathbf{f} = \mathbf{0}. \quad (43)$$

Knowing the solution \mathbf{q}_n at time $t = t_n$ we want to get the change in the solution $\Delta\mathbf{q}$ due to the change in the load function from \mathbf{f}_n to

$$\mathbf{f}_{n+1} = \mathbf{f}_n + \Delta\mathbf{f}. \quad (44)$$

The change in the solution according

$$\mathbf{q}_{n+1} = \mathbf{q}_n + \Delta\mathbf{q}. \quad (45)$$

will be achieved by using a sequence of successive approximations to \mathbf{q}_{n+1} which are denoted by $\mathbf{q}_{n+1}^{(k+1)}$. Here k is the iteration counter starting from

$$\mathbf{q}_{n+1}^{(1)} = \mathbf{q}_n \quad (46)$$

The successive approximations can be written as

$$\mathbf{q}_{n+1}^{(k+1)} = \mathbf{q}_n + \Delta\mathbf{q}^{(k+1)} = \mathbf{q}_{n+1}^{(k)} + d\mathbf{q}^{(k+1)}, \quad (47)$$

where

$$\Delta\mathbf{q}^{(k+1)} = \sum_{j=1}^k d\mathbf{q}^{(j+1)}. \quad (48)$$

Using the Newton-Raphson method we calculate the successive approximations $d\mathbf{q}^{(k+1)}$ from

$$\frac{\partial\mathbf{F}(\mathbf{q} = \mathbf{q}^{(k)})}{\partial\mathbf{q}} d\mathbf{q}^{(k+1)} = \mathbf{f} - \mathbf{F}(\mathbf{q}^{(k)}) \quad (49)$$

where for the k -th iteration we define the global tangent stiffness matrix as

$$\mathbf{K}_T^{(k)} = \frac{\partial\mathbf{F}(\mathbf{q} = \mathbf{q}^{(k)})}{\partial\mathbf{q}} \quad (50)$$

For notational simplification, in equation (49) the time step indicator $(n+1)$ has been omitted as an additional index for \mathbf{F} , $d\mathbf{q}$, \mathbf{q} and \mathbf{f} .

At the element level the successive approximations for achieving convergence to the state at $t = t_{n+1}$ due to a change in the external load from t_n to t_{n+1} can be characterized as

$$\begin{aligned}
 \tilde{\mathbf{u}}_{n+1}^{(k+1)} &= \tilde{\mathbf{u}}_{n+1}^{(k)} + \Delta\tilde{\mathbf{u}}^{(k+1)} \\
 \boldsymbol{\varepsilon}_{n+1}^{(k+1)} &= \boldsymbol{\varepsilon}_{n+1}^{(k)} + \Delta\boldsymbol{\varepsilon}^{(k+1)} \\
 \boldsymbol{\varepsilon}_{n+1}^i{}^{(k+1)} &= \boldsymbol{\varepsilon}_{n+1}^i{}^{(k)} + \Delta\boldsymbol{\varepsilon}^i{}^{(k+1)} \\
 \boldsymbol{\sigma}_{n+1}^{(k+1)} &= \boldsymbol{\sigma}_{n+1}^{(k)} + \Delta\boldsymbol{\sigma}^{(k+1)} \\
 \left[\frac{\partial \mathbf{W}}{\partial \boldsymbol{\varepsilon}} \right]_{n+1}^{(k+1)} &= \boldsymbol{\sigma}_{n+1}^{(k)} + \Delta\tilde{\boldsymbol{\sigma}}^{(k+1)}.
 \end{aligned} \tag{51}$$

The initial values in the iteration process are

$$\begin{aligned}
 \tilde{\mathbf{u}}_{n+1}^{(1)} &= \tilde{\mathbf{u}}_n \\
 \boldsymbol{\varepsilon}_{n+1}^{(1)} &= \boldsymbol{\varepsilon}_n \\
 \boldsymbol{\varepsilon}_{n+1}^i{}^{(1)} &= \boldsymbol{\varepsilon}_n^i \\
 \boldsymbol{\sigma}_{n+1}^{(1)} &= \boldsymbol{\sigma}_n
 \end{aligned} \tag{52}$$

As a result of the linearization process of the non-linear constitutive model we get for every iteration k an incremental stress-strain relationship of the form

$$\Delta\tilde{\boldsymbol{\sigma}}^{(k+1)}(\mathbf{x}) = \mathbf{E}_{\mathbf{T}}(\mathbf{x}, \boldsymbol{\varepsilon}^{(k)}(\mathbf{x})) \Delta\boldsymbol{\varepsilon}^{(k+1)}(\mathbf{x}) \tag{53}$$

which can be used in equation (51₅). The algorithmic tangent moduli $\mathbf{E}_{\mathbf{T}}$ are computed at every Gauss-point for each finite element.

Here we restrict ourselves to show the structure of the tangent stiffness matrix of an element and the element residual vector. For the derivation of the algorithmic tangent moduli $\mathbf{E}_{\mathbf{T}}$ we refer to the literature [12-18].

For the finite element approximation of the increments at time step $(n+1)$ and iteration $(k+1)$ we choose the following discrete fields:

$$\begin{aligned}
 \Delta\tilde{\mathbf{u}} &= \mathbf{N}d\mathbf{q} \\
 \Delta\boldsymbol{\varepsilon} &= \mathbf{A}d\boldsymbol{\alpha} \\
 \Delta\boldsymbol{\sigma} &= \mathbf{E}d\boldsymbol{\beta} = \mathbf{P}d\boldsymbol{\beta} \\
 \Delta\boldsymbol{\varepsilon}^i &= \mathbf{B}^i d\boldsymbol{\lambda}
 \end{aligned} \tag{54}$$

where $d\mathbf{q}$ is the increment of nodal displacements of the finite element under consideration. Note the iteration counter $(k+1)$ and the load step indicator $(n+1)$ are omitted in

the definition of the incremental fields (54). Again we choose $\mathbf{A} = \mathbf{D}\mathbf{U}$ and $\mathbf{P} = \mathbf{E}\mathbf{A} = \mathbf{E}\mathbf{D}\mathbf{U}$. The strain field $\Delta\boldsymbol{\varepsilon}$ is derived from a displacement field $\Delta\mathbf{u}$ which is given by

$$\Delta\mathbf{u} = \mathbf{U}d\alpha \quad (55)$$

The incremental strains $\Delta(\mathbf{D}\tilde{\mathbf{u}})$ are given by

$$\Delta(\mathbf{D}\tilde{\mathbf{u}}) = \mathbf{D}\mathbf{N}d\mathbf{q} = \mathbf{B}d\mathbf{q} \quad (56)$$

The displacement field $\Delta\mathbf{u}$ is constructed such that it satisfies the Navier-equations (25) which are the governing differential equations for the linear elastic case. This choice for $\Delta\mathbf{u}$ is motivated by the aim to recover the equations of section 3 for the special case that our material becomes linear elastic.

From the modified Hu-Washizu functional (2) we get the following four equations:

$$-\int_{\mathbf{V}} \delta\boldsymbol{\sigma}^T \left[\boldsymbol{\varepsilon} - \mathbf{D}\tilde{\mathbf{u}} - \boldsymbol{\varepsilon}^i \right] dV = 0 \quad (57)$$

$$\int_{\mathbf{V}} \delta\boldsymbol{\varepsilon}^T \left[\frac{\partial W}{\partial \boldsymbol{\varepsilon}} - \boldsymbol{\sigma} \right] dV = 0 \quad (58)$$

$$\int_{\mathbf{V}} \delta(\mathbf{D}\tilde{\mathbf{u}})^T \boldsymbol{\sigma} dV = \int_{\mathbf{V}} \delta\tilde{\mathbf{u}}^T \bar{\mathbf{f}} dV + \int_{\mathbf{S}} \delta\tilde{\mathbf{u}}^T \bar{\mathbf{T}} dS \quad (59)$$

$$\int_{\mathbf{V}} (\delta\boldsymbol{\varepsilon}^i)^T \boldsymbol{\sigma} dV = 0 \quad (60)$$

Now the equations (57)-(60) are used for the evaluation of the physical quantities at t_{n+1} .

Using equations (51), (53), (54), and (56) we substitute the expressions for $\tilde{\mathbf{u}} = \tilde{\mathbf{u}}_{n+1}^{(k+1)}$,

$\boldsymbol{\varepsilon} = \boldsymbol{\varepsilon}_{n+1}^{(k+1)}$, $\boldsymbol{\varepsilon}^i = \boldsymbol{\varepsilon}_{n+1}^{i(k+1)}$, $\boldsymbol{\sigma} = \boldsymbol{\sigma}_{n+1}^{(k+1)}$, $\frac{\partial W}{\partial \boldsymbol{\varepsilon}} = \left[\frac{\partial W}{\partial \boldsymbol{\varepsilon}} \right]_{n+1}^{(k+1)}$ into (57)-(60) and make use of the relations

$$\begin{aligned} \delta\boldsymbol{\sigma}_{n+1}^{(k+1)} &= \delta(\Delta\boldsymbol{\sigma}^{(k+1)}) \\ \delta\boldsymbol{\varepsilon}_{n+1}^{(k+1)} &= \delta(\Delta\boldsymbol{\varepsilon}^{(k+1)}) \\ \delta\boldsymbol{\varepsilon}_{n+1}^{i(k+1)} &= \delta(\Delta\boldsymbol{\varepsilon}^{i(k+1)}) \\ \delta(\mathbf{D}\tilde{\mathbf{u}}_{n+1}^{(k+1)}) &= \delta(\mathbf{D}\Delta\tilde{\mathbf{u}}^{(k+1)}) \end{aligned} \quad (61)$$

Omitting the indices (n+1) and (k+1) this gives us the following set of equations:

$$-\delta d\boldsymbol{\beta}^T \int_{\mathbf{V}} \left[\mathbf{P}^T \mathbf{A} \alpha - \mathbf{P}^T \mathbf{B} d\mathbf{q} - \mathbf{P}^T \mathbf{B}^i d\lambda \right] dV = 0$$

$$\delta d\alpha^T \int_V \left[\mathbf{A}^T \mathbf{E}_T \mathbf{A} \alpha - \mathbf{A}^T \mathbf{P} \beta \right] dV = 0 \quad (62)$$

$$\delta d\mathbf{q}^T \int_V \mathbf{B}^T \mathbf{P} dV d\beta = \delta d\mathbf{q}^T \left[\mathbf{f}_{\text{ext.}} - \mathbf{f}_{\text{int}} \right]$$

$$\delta d\lambda^T \int_V \mathbf{B}^{iT} \mathbf{P} dV d\beta = \delta d\lambda^T \left[\mathbf{0} - \mathbf{f}_{\text{int}}^i \right]$$

where the residual vectors are

$$\mathbf{f}_{\text{int}} = \int_V \mathbf{B}^T \boldsymbol{\sigma}_{n+1}^{(k)} dV \quad (63)$$

$$\mathbf{f}_{\text{int}}^i = \int_V \mathbf{B}^{iT} \boldsymbol{\sigma}_{n+1}^{(k)} dV.$$

We recall that the matrices \mathbf{A} and \mathbf{P} , containing the assumed strain and stress terms, are constructed from a displacement matrix \mathbf{U} according equations (55), (23) and (24). Utilizing that $\mathbf{P} = \mathbf{E}\mathbf{A}$ and $\mathbf{A} = \mathbf{E}^{-1}\mathbf{P}$ we get from (62) the following system of equations

$$\begin{bmatrix} \mathbf{0} & -\mathbf{H} & \mathbf{L} & \mathbf{L}^i \\ -\mathbf{H} & \mathbf{H}_T & \mathbf{0} & \mathbf{0} \\ \mathbf{L}^T & \mathbf{0} & \mathbf{0} & \mathbf{0} \\ \mathbf{L}^{iT} & \mathbf{0} & \mathbf{0} & \mathbf{0} \end{bmatrix}^{(k)} \begin{bmatrix} d\beta \\ d\alpha \\ d\mathbf{q} \\ d\lambda \end{bmatrix}^{(k+1)} = \begin{bmatrix} \mathbf{0} \\ \mathbf{0} \\ \mathbf{f}_{\text{ext}} \\ \mathbf{0} \end{bmatrix}^{(k+1)} - \begin{bmatrix} \mathbf{0} \\ \mathbf{0} \\ \mathbf{f}_{\text{int}} \\ \mathbf{f}_{\text{int}}^i \end{bmatrix}^{(k)} \quad (64)$$

where

$$\mathbf{H}_T = \int_V \mathbf{A}^T \mathbf{E}_T \mathbf{A} dV \quad (65)$$

The matrices \mathbf{H} , \mathbf{L} , \mathbf{L}^i and the vector \mathbf{f}_{ext} are the same as in the linear elastic case and they are given with equations (29).

From the first two equations of (64) we obtain the strain and stress parameters as

$$d\alpha = \mathbf{H}^{-1} \mathbf{L} d\mathbf{q} + \mathbf{H}^{-1} \mathbf{L}^i d\lambda \quad (66)$$

$$d\beta = \mathbf{H}^{-1} \mathbf{H}_T \alpha = \mathbf{H}^{-1} \mathbf{H}_T \mathbf{H}^{-1} \mathbf{L} d\mathbf{q} + \mathbf{H}^{-1} \mathbf{H}_T \mathbf{H}^{-1} \mathbf{L}^i d\lambda. \quad (67)$$

Substitution of (66) and (67) into the last two equations of (64) gives us the following system of equations:

$$\begin{bmatrix} \mathbf{L}^T \mathbf{H}^{-1} \mathbf{H}_T \mathbf{H}^{-1} \mathbf{L} & \mathbf{L}^T \mathbf{H}^{-1} \mathbf{H}_T \mathbf{H}^{-1} \mathbf{L}^i \\ \mathbf{L}^{iT} \mathbf{H}^{-1} \mathbf{H}_T \mathbf{H}^{-1} \mathbf{L} & \mathbf{L}^{iT} \mathbf{H}^{-1} \mathbf{H}_T \mathbf{H}^{-1} \mathbf{L}^i \end{bmatrix} \begin{bmatrix} d\mathbf{q} \\ d\lambda \end{bmatrix} = \begin{bmatrix} \mathbf{f}_{\text{ext}} \\ \mathbf{0} \end{bmatrix} - \begin{bmatrix} \mathbf{f}_{\text{int}} \\ \mathbf{f}_{\text{int}}^i \end{bmatrix} \quad (68)$$

Using the submatrices

$$\begin{aligned}
 \mathbf{K}_T &= \mathbf{L}^T \mathbf{H}^{-1} \mathbf{H}_T \mathbf{H}^{-1} \mathbf{L} \\
 \Gamma_T &= \mathbf{L}^{iT} \mathbf{H}^{-1} \mathbf{H}_T \mathbf{H}^{-1} \mathbf{L} \\
 \mathbf{Q}_T &= \mathbf{L}^{iT} \mathbf{H}^{-1} \mathbf{H}_T \mathbf{H}^{-1} \mathbf{L}^i
 \end{aligned} \tag{69}$$

we get from the condensation process the element tangent stiffness matrix in the form

$$\mathbf{k}_T = \mathbf{K}_T - \Gamma_T^T \mathbf{Q}_T^{-1} \Gamma_T \tag{70}$$

In the case that the material is linear elastic we have

$$\mathbf{H}_T = \mathbf{H} \tag{71}$$

so that the equations (33) - (35) will be recovered.

The element equations for the k-th iteration are now written in the form

$$\mathbf{k}_T^{(k)} d\mathbf{q}^{(k+1)} = \mathbf{r}^{(k+1)} \tag{72}$$

where

$$\mathbf{r}^{(k+1)} = \mathbf{f}_{\text{ext}}^{(k+1)} - \left[\mathbf{f}_{\text{int}} - \Gamma_T^T \mathbf{Q}_T^{-1} \mathbf{f}_{\text{int}}^i \right]^{(k)}. \tag{73}$$

After assembling all element equations we can solve the linear system of equations for the incremental nodal displacements and update the nodal displacements as indicated in equation (47). Once the incremental nodal displacements are calculated we can compute for every element the vector of incremental enhanced strain parameters $d\boldsymbol{\lambda}^{(k+1)}$, which is obtained from

$$d\boldsymbol{\lambda}^{(k+1)} = - \left[\mathbf{Q}_T^{-1} \Gamma_T \right]^{(k)} d\mathbf{q}^{(k+1)} - \left[\mathbf{Q}_T^{-1} \mathbf{f}_{\text{int}}^i \right]^{(k)} \tag{74}$$

The update of the enhanced strain parameters for each finite element follows with the aid of

$$\boldsymbol{\lambda}^{(k+1)} = \boldsymbol{\lambda}^{(k)} + d\boldsymbol{\lambda}^{(k+1)} \tag{75}$$

In order to avoid computing matrices and vectors from the k-th iteration again after the computation of the nodal displacements $d\mathbf{q}^{(k+1)}$ is already finished, we save the arrays $\left[\mathbf{Q}_T^{-1} \Gamma_T \right]^{(k)}$ and $\left[\mathbf{Q}_T^{-1} \mathbf{f}_{\text{int}}^i \right]^{(k)}$ along with other history data during the process of assembling the equations for the unknowns $d\mathbf{q}^{(k+1)}$. This way the enhanced strain parameters $d\boldsymbol{\lambda}^{(k+1)}$ from equation (74) can be obtained without computing arrays which have already been used before.

5. Systematic construction of the displacement, stress and strain fields

For the fields \mathbf{u} , ε and σ we want to choose linearly independent functions which satisfy the governing differential equations for the linear elastic case. A systematic way of deriving complete polynomials of a given order is to use complex function representations which are available for two- and three-dimensional elasticity problems [19-24]. For plane strain and plane stress we can use the Kolosov-Muskhelishvili representation [24] given by

$$\begin{aligned}
 2\mu u &= \text{Re}[\kappa\Phi(z) - z\overline{\Phi'(z)} - \overline{\Psi(z)}] \\
 2\mu v &= \text{Im}[\kappa\Phi(z) - z\overline{\Phi'(z)} - \overline{\Psi(z)}] \\
 \sigma_{xx} &= \text{Re}[2\Phi'(z) - \bar{z}\Phi''(z) - \Psi'(z)] \\
 \sigma_{yy} &= \text{Re}[2\Phi'(z) + \bar{z}\Phi''(z) + \Psi'(z)] \\
 \tau_{xy} &= \text{Im}[\bar{z}\Phi''(z) + \Psi'(z)]
 \end{aligned} \tag{76}$$

where

$$\begin{aligned}
 z &= x + iy, \\
 2\mu &= E/(1 + \nu) \\
 \kappa &= \begin{cases} (3 - \nu)/(1 + \nu) & \text{for plane stress} \\ (3 - 4\nu) & \text{for plane strain} \end{cases}
 \end{aligned} \tag{77}$$

The complex functions are chosen in the form

$$\begin{aligned}
 \Phi(z) &= \sum_{j=1}^N (a_j + ib_j)z^j \\
 \Psi(z) &= \sum_{j=0}^N (c_j + id_j)z^j
 \end{aligned} \tag{78}$$

The advantage of using a complex representation are

- (i) We get functions which are complete up to the chosen order N and they are invariant with respect to coordinate translations and rotations.
- (ii) We obtain stresses which satisfy not only the equilibrium equations but also the compatibility equations.

For the four node element we will use quadratic displacements $\mathbf{u} = \mathbf{U}\boldsymbol{\beta}$. Choosing $N=2$, we get ten terms for our fields. The matrix \mathbf{U}^T in this case is given by

$$2\mu\mathbf{U}^T = \begin{bmatrix} 1 & 0 \\ 0 & 1 \\ (\kappa-1)x & (\kappa-1)y \\ -(\kappa+1)y & (\kappa+1)x \\ -x & y \\ y & x \\ \kappa(x^2-y^2) - 2(x^2+y^2) & 2\kappa xy \\ -2\kappa xy & \kappa(x^2-y^2) + 2(x^2+y^2) \\ y^2-x^2 & 2xy \\ 2xy & y^2-x^2 \end{bmatrix} \quad (79)$$

The according stresses are

$$\boldsymbol{\sigma} = \begin{bmatrix} \sigma_{xx} \\ \sigma_{yy} \\ \tau_{xy} \end{bmatrix} = \begin{bmatrix} 0 & 0 & 2 & 0 & -1 & 0 & 2x & -6y & -2x & 2y \\ 0 & 0 & 2 & 0 & 1 & 0 & 6x & -2y & 2x & -2y \\ 0 & 0 & 0 & 0 & 0 & 1 & -2y & 2x & 2y & 2x \end{bmatrix} \begin{bmatrix} \beta \end{bmatrix} \quad (80)$$

For the computation of the element stiffness matrix we have to omit the terms which are associated to rigid body modes. Therefore seven linearly independent stress and strain vectors will be left in our example of a four node element.

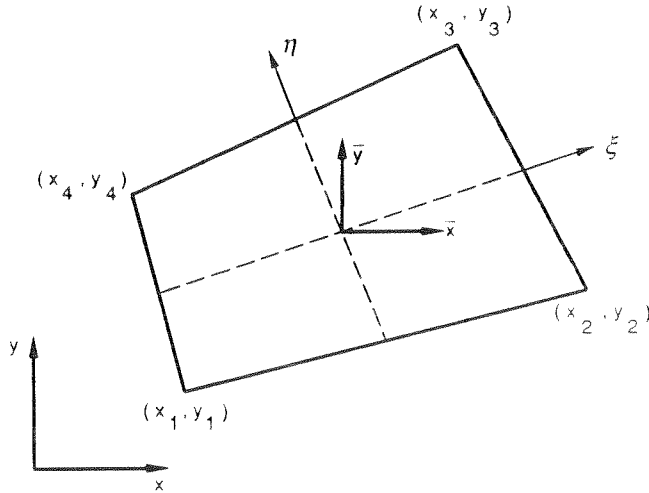


Figure 1: Coordinates for a four-node element

Instead of choosing the stresses and strains in global cartesian coordinates x, y we can choose them in local cartesian coordinates \bar{x}, \bar{y} (Figure 1). The relationship between the cartesian coordinates and the natural coordinates ξ, η are given by

$$\begin{aligned} x &= a_0 + a_1\xi + a_2\eta + a_3\xi\eta \\ y &= b_0 + b_1\xi + b_2\eta + b_3\xi\eta \\ \bar{x} &= x - a_0 \end{aligned} \quad (81)$$

$$\bar{y} = y - b_0$$

where

$$\begin{aligned} a_0 &= \frac{1}{4} (x_1 + x_2 + x_3 + x_4), & b_0 &= \frac{1}{4} (y_1 + y_2 + y_3 + y_4), \\ a_1 &= \frac{1}{4} (-x_1 + x_2 + x_3 - x_4), & b_1 &= \frac{1}{4} (-y_1 + y_2 + y_3 - y_4), \\ a_2 &= \frac{1}{4} (-x_1 - x_2 + x_3 + x_4), & b_2 &= \frac{1}{4} (-y_1 - y_2 + y_3 + y_4), \\ a_3 &= \frac{1}{4} (x_1 - x_2 + x_3 - x_4), & b_3 &= \frac{1}{4} (y_1 - y_2 + y_3 - y_4), \end{aligned} \tag{82}$$

Substitution of (81) into the assumed stresses $\sigma(\bar{x}, \bar{y})$ gives us the stresses in terms of the natural coordinates ξ, η .

Denoting the column vectors of the matrix \mathbf{P} by \mathbf{P}_j the stresses can be written in the form

$$\sigma = \left[\mathbf{P}_1 \mathbf{P}_2 \mathbf{P}_3 \mathbf{P}_4 \mathbf{P}_5 \mathbf{P}_6 \mathbf{P}_7 \right] \left[\beta \right] \tag{83}$$

By forming linear combinations of the linearly independent vectors \mathbf{P}_j it is possible to find other vectors $\hat{\mathbf{P}}_j$ which are also linearly independent. Such a process would result into another form for our stress assumption:

$$\sigma = \left[\hat{\mathbf{P}}_1 \hat{\mathbf{P}}_2 \hat{\mathbf{P}}_3 \hat{\mathbf{P}}_4 \hat{\mathbf{P}}_5 \hat{\mathbf{P}}_6 \hat{\mathbf{P}}_7 \right] \left[\hat{\beta} \right] \tag{84}$$

The optimal form of arranging the stress terms in the matrix \mathbf{P} would be the one which leads to a diagonal matrix \mathbf{H} , since \mathbf{H} has to be inverted. Starting with a given system of stress vectors \mathbf{P}_j we can construct a system of vectors $\hat{\mathbf{P}}_j$ which are orthogonal to each other in the following sense

$$\int_v \mathbf{P}_i^T \mathbf{E}^{-1} \mathbf{P}_j \, dV \begin{cases} = 0 & \text{for } i \neq j \\ \neq 0 & \text{for } i = j \end{cases} \tag{85}$$

This can be achieved by a Gram-Schmidt-orthogonalization process which in our case would be performed as follows:

$$\hat{\mathbf{P}}_j = \mathbf{P}_j - \sum_{k=1}^{j-1} \frac{\int_v \mathbf{P}_j^T \mathbf{E}^{-1} \hat{\mathbf{P}}_k \, dV}{\int_v \hat{\mathbf{P}}_k^T \mathbf{E}^{-1} \hat{\mathbf{P}}_k \, dV} \hat{\mathbf{P}}_k \tag{86}$$

All integrals in the above process are scalar quantities and can be calculated analytically

after transforming the integrands to natural coordinates. For the evaluation of the integrals in equation (86) we need the Jacobian \mathbf{J} of the transformations (81), which is given by

$$\mathbf{J} = \det \mathbf{J} = J_0 + J_1\xi + J_2\eta \quad (87)$$

where

$$\mathbf{J} = \begin{bmatrix} x_\xi & y_\xi \\ x_\eta & y_\eta \end{bmatrix} \quad (88)$$

and

$$\begin{aligned} J_0 &= a_1b_2 - a_2b_1 \\ J_1 &= a_1b_3 - b_1a_3 \\ J_2 &= a_3b_2 - a_2b_3 \end{aligned} \quad (89)$$

The values of \mathbf{J}_0 and J_0 are defined as $\mathbf{J}_0 = \mathbf{J}(0, 0)$, and $J_0 = J(0, 0)$. The coefficients a_j and b_j are given with equations (82). Symbolic manipulation programs such as MACSYMA or MATHEMATICA can be used for a convenient evaluation of the integrals in (86).

A partial orthogonalization was used to keep the expressions for the matrix entries of \mathbf{P} simple. Choosing the stresses

$$\boldsymbol{\sigma} = \begin{bmatrix} \sigma_{xx} \\ \sigma_{yy} \\ \tau_{xy} \end{bmatrix} = \begin{bmatrix} 2 & -1 & 0 & \bar{x} - \bar{x}_0 & -3(\bar{y} - \bar{y}_0) & -(\bar{x} - \bar{x}_0) & \bar{y} - \bar{y}_0 \\ 2 & 1 & 0 & 3(\bar{x} - \bar{x}_0) & -(\bar{y} - \bar{y}_0) & \bar{x} - \bar{x}_0 & -(\bar{y} - \bar{y}_0) \\ 0 & 0 & 1 & -(\bar{y} - \bar{y}_0) & \bar{x} - \bar{x}_0 & \bar{y} - \bar{y}_0 & \bar{x} - \bar{x}_0 \end{bmatrix} \begin{bmatrix} \beta \end{bmatrix} \quad (90)$$

where

$$\bar{x}_0 = \frac{a_2J_2 + a_1J_1}{3J_0} \quad (91)$$

$$\bar{y}_0 = \frac{b_2J_2 + b_1J_1}{3J_0}$$

we obtain the following structure for the matrix \mathbf{H} :

$$\mathbf{H} = \begin{bmatrix} \mathbf{H}_{11} & \mathbf{0} \\ \mathbf{0} & \mathbf{H}_{22} \end{bmatrix} \quad (92)$$

where the diagonal matrix \mathbf{H}_{11} is given by

$$\mathbf{H}_{11} = \frac{J_0 t}{E} \begin{bmatrix} 32(1-\nu) & 0 & 0 \\ 0 & 8(1+\nu) & 0 \\ 0 & 0 & 8(1+\nu) \end{bmatrix} \quad (93)$$

for plane stress, and

$$\mathbf{H}_{11} = \frac{J_0 (1 + \nu)t}{E} \begin{bmatrix} 32(1 - 2\nu) & 0 & 0 \\ 0 & 8 & 0 \\ 0 & 0 & 8 \end{bmatrix} \quad (94)$$

for plane strain. The values for J_0 , J_1 and J_2 are given with relation (89). The thickness of the plate is denoted by t . The symmetric 4x4 matrix \mathbf{H}_{22} is integrated numerically.

For the strains we obtain according the explanations in section 3

$$\boldsymbol{\varepsilon} = \begin{bmatrix} \varepsilon_{xx} \\ \varepsilon_{yy} \\ \gamma_{xy} \end{bmatrix} = \frac{1}{2\mu} \begin{bmatrix} (\kappa - 1) & -1 & 0 & (\kappa - 2)(\bar{x} - \bar{x}_0) & -\kappa(\bar{y} - \bar{y}_0) & -(\bar{x} - \bar{x}_0) & \bar{y} - \bar{y}_0 \\ (\kappa - 1) & 1 & 0 & \kappa(\bar{x} - \bar{x}_0) & -(\kappa - 2)(\bar{y} - \bar{y}_0) & \bar{x} - \bar{x}_0 & -(\bar{y} - \bar{y}_0) \\ 0 & 0 & 2 & -2(\bar{y} - \bar{y}_0) & 2(\bar{x} - \bar{x}_0) & 2(\bar{y} - \bar{y}_0) & 2(\bar{x} - \bar{x}_0) \end{bmatrix} \begin{bmatrix} \boldsymbol{\beta} \end{bmatrix} \quad (95)$$

It should be noted that after substituting (\bar{x}, \bar{y}) and (\bar{x}_0, \bar{y}_0) into (90) and (95) the assumed strains and stresses, in addition to the constant terms, involve the terms ξ , η , $\xi\eta$.

For the four-node element the compatible displacement field $\tilde{\mathbf{u}}$ is interpolated with standard shape functions according

$$\tilde{\mathbf{u}} = \begin{bmatrix} \tilde{u} \\ \tilde{v} \end{bmatrix} = \sum_{i=1}^4 (1 + \xi_i \xi)(1 + \eta_i \eta) \begin{bmatrix} u_i \\ v_i \end{bmatrix} = \mathbf{N}\mathbf{q} \quad (96)$$

where u_i , v_i are the nodal displacements and ξ_i , η_i denote the location of the element nodes in natural coordinates.

6. Selection of enhanced strain modes

In order to avoid the derivation of an overly stiff element one should choose a minimum number of stress and strain terms. For the four-node element the number of nodal displacements is $n_q = 8$. From

$$n_\beta \geq n_q - r, \quad (97)$$

where r is the number of rigid body modes, we obtain the optimal number of stress terms as $n_\beta = 5$. However, if we choose five stress terms in cartesian coordinates, the assumed stress field will be an incomplete linear field and the resulting element will not be invariant with respect to the choice of the coordinates' frame.

The use of a complete linear stress field in cartesian coordinates, consisting of seven terms, leads to an element which tends to be stiffer than the five parameter hybrid

stress element of Pian/Sumihara, which is formulated in natural coordinates. In order to be able to use the seven parameter stress field (90) formulated in cartesian coordinates, we have to add additional degrees of freedom n_λ to the element. Using enhanced strain modes or incompatible displacements as additional unknowns, the requirement for the number of stress terms becomes

$$n_\beta = (n_q + n_\lambda) - r \quad (98)$$

If we want to use the seven parameter stress field (90) for the four-node element (for which we have $n_q = 8$ and $r = 3$) we have to choose the additional number of element unknowns as $n_\lambda = 2$ in order to achieve optimal performance of the element.

In a recent paper by Simo and Rifai [3] different forms of enhanced strain fields are discussed. Here we want to consider two types of enhanced strain functions which have been proposed in the literature and try to utilize them for the present four-node element.

6.1 First set of enhanced strain functions

The first set of enhanced strain functions was given by Taylor/Beresford/Wilson [2] in 1976. The proposed enhanced strain terms were constructed from the incompatible shape functions

$$N_1^i = 1 - \xi^2 \quad (99)$$

and

$$N_2^i = 1 - \eta^2 \quad (100)$$

Instead of calculating the strains from the gradient

$$\nabla N_j^i = \begin{bmatrix} \frac{\partial}{\partial x} \\ \frac{\partial}{\partial y} \end{bmatrix} N_j^i = \frac{1}{J(\xi, \eta)} \begin{bmatrix} y_\eta(\xi, \eta) & -y_\xi(\xi, \eta) \\ -x_\eta(\xi, \eta) & x_\xi(\xi, \eta) \end{bmatrix} \begin{bmatrix} \frac{\partial}{\partial \xi} \\ \frac{\partial}{\partial \eta} \end{bmatrix} N_j^i = \mathbf{J}^{-1}(\xi, \eta) \begin{bmatrix} \frac{\partial}{\partial \xi} \\ \frac{\partial}{\partial \eta} \end{bmatrix} N_j^i \quad (101)$$

the approximated gradient

$$\nabla_0 N_j^i = \frac{1}{J(\xi, \eta)} \begin{bmatrix} y_\eta(0, 0) & -y_\xi(0, 0) \\ -x_\eta(0, 0) & x_\xi(0, 0) \end{bmatrix} \begin{bmatrix} \frac{\partial}{\partial \xi} \\ \frac{\partial}{\partial \eta} \end{bmatrix} N_j^i = \frac{J_0}{J(\xi, \eta)} \mathbf{J}_0^{-1} \begin{bmatrix} \frac{\partial}{\partial \xi} \\ \frac{\partial}{\partial \eta} \end{bmatrix} N_j^i \quad (102)$$

was used. The Jacobian matrix \mathbf{J} and its determinant J are given in equations (87) - (89). The values of \mathbf{J}_0 and J_0 are defined as $\mathbf{J}_0 = \mathbf{J}(0, 0)$, and $J_0 = J(0, 0)$. Using the shape functions (99) and (100) for the incompatible displacement field

$$\mathbf{u}^i = \begin{bmatrix} N_1^i & N_2^i & 0 & 0 \\ 0 & 0 & N_1^i & N_2^i \end{bmatrix} \begin{bmatrix} \lambda_1 \\ \lambda_2 \\ \lambda_3 \\ \lambda_4 \end{bmatrix} \quad (103)$$

and the approximated gradient operator (102) we get the following strain field

$$\boldsymbol{\varepsilon}^i = \begin{bmatrix} \varepsilon_{xx}^i \\ \varepsilon_{yy}^i \\ \gamma_{xy}^i \end{bmatrix} = \frac{2}{J(\xi, \eta)} \begin{bmatrix} -b_2\xi & b_1\eta & 0 & 0 \\ 0 & 0 & a_2\xi & -a_1\eta \\ a_2\xi & -a_1\eta & -b_2\xi & b_1\eta \end{bmatrix} \begin{bmatrix} \lambda_1 \\ \lambda_2 \\ \lambda_3 \\ \lambda_4 \end{bmatrix} \quad (104)$$

The above constructed strain field (104) is orthogonal to the chosen reference stresses and satisfies therefore equation (15). The reference stresses $\boldsymbol{\sigma}^*$ are chosen as

$$\boldsymbol{\sigma}^* = \mathbf{F}_0 \boldsymbol{\Sigma} \quad (105)$$

where

$$\boldsymbol{\Sigma} = \mathbf{P}^* \boldsymbol{\beta}^*$$

$$\mathbf{P}^* = \begin{bmatrix} 1 & 0 & 0 & \xi & 0 \\ 0 & 1 & 0 & 0 & \eta \\ 0 & 0 & 1 & 0 & 0 \end{bmatrix} \quad (106)$$

$$\mathbf{F}_0 = \begin{bmatrix} J_{11}^2 & J_{12}^2 & 2J_{11}J_{12} \\ J_{21}^2 & J_{22}^2 & 2J_{22}J_{21} \\ J_{11}J_{21} & J_{12}J_{22} & (J_{11}J_{22} + J_{12}J_{21}) \end{bmatrix} (\xi = 0, \eta = 0)$$

and

$$\begin{bmatrix} J_{11} & J_{12} \\ J_{21} & J_{22} \end{bmatrix} = \begin{bmatrix} x_\xi & y_\xi \\ x_\eta & y_\eta \end{bmatrix} \quad (107)$$

The matrix \mathbf{F}_0 in equation (105) maps the local stresses, $\boldsymbol{\Sigma}$, from the isoparametric space to the physical stresses, $\boldsymbol{\sigma}^{*T} = [\sigma_{xx}^* \sigma_{yy}^* \tau_{xy}^*]$, in the global frame. The mapping (105) can be derived from the tensor transformation

$$\sigma_{ij}^* = J_{iA} \Sigma_{AB} J_{jB} \quad (108)$$

if we evaluate the coefficients J_{AB} at the center of the element.

6.2 Second set of enhanced strain functions

The second set of enhanced strains can be obtained by choosing for \mathbf{u}^i in equation (103) the following incompatible displacement functions [25,26]:

$$N_1^i = \left(1 - \frac{J_2}{J_0} \eta\right)(1 - \xi^2) + \frac{J_1}{J_0} \xi(1 - \eta^2) \quad (109)$$

$$N_2^i = \left(1 - \frac{J_1}{J_0} \xi\right)(1 - \eta^2) + \frac{J_2}{J_0} \eta(1 - \xi^2)$$

The above incompatible shape functions vanish at the nodal points of the element. The use of the incompatible displacement functions (103) and the exact gradient operator (101) leads to the enhanced strain field

$$\boldsymbol{\varepsilon}^i = \begin{bmatrix} \varepsilon_{xx}^i \\ \varepsilon_{yy}^i \\ \gamma_{xy}^i \end{bmatrix} = \begin{bmatrix} N_{1,x}^i & N_{2,x}^i & 0 & 0 \\ 0 & 0 & N_{1,y}^i & N_{2,y}^i \\ N_{1,y}^i & N_{2,y}^i & N_{1,x}^i & N_{2,x}^i \end{bmatrix} \begin{bmatrix} \lambda_1 \\ \lambda_2 \\ \lambda_3 \\ \lambda_4 \end{bmatrix} \quad (110)$$

where

$$N_{j,x}^i = \frac{1}{J(\xi, \eta)} \left[(b_2 + b_3 \xi) N_{j,\xi}^i - (b_1 + b_3 \eta) N_{j,\eta}^i \right] \quad (111)$$

$$N_{j,y}^i = \frac{1}{J(\xi, \eta)} \left[-(a_2 + a_3 \xi) N_{j,\xi}^i + (a_1 + a_3 \eta) N_{j,\eta}^i \right]$$

Performing the differentiation of the functions (109) with respect to the natural coordinates we obtain expressions for the strains $\boldsymbol{\varepsilon}^i$ which are more lengthy than the enhanced strains in equation (104).

6.3 Enhanced strains used for the numerical examples

Both enhanced strain fields described above contain four parameters. For the proposed element with seven stress terms we need an enhanced strain field with only two parameters. In order to find two enhanced strain modes which are suitable for our case, linear combinations of incompatible shape functions are used and the incompatible displacement field is redefined in the following form

$$\mathbf{u}^i = \begin{bmatrix} \frac{1}{2} (N_1^i - N_2^i) & 0 & \frac{1}{2} (N_1^i + N_2^i) & 0 \\ 0 & \frac{1}{2} (N_1^i - N_2^i) & 0 & \frac{1}{2} (N_1^i + N_2^i) \end{bmatrix} \begin{bmatrix} \lambda_1 \\ \lambda_2 \\ \lambda_3 \\ \lambda_4 \end{bmatrix} \quad (112)$$

For both types of enhanced strain fields (i.e. using i) shape functions (99),(100) in connection with the approximated gradient operator (102) and ii) shape functions (109) in connection with the gradient operator (101)), we find that the terms associated with λ_3 and λ_4 cannot be used since the according strain terms are orthogonal to all stresses defined

in (90) and lead to a vanishing matrix \mathbf{L}^i . The terms associated with λ_1 and λ_2 will give us a matrix \mathbf{L}^i with the following structure:

$$\mathbf{L}^i = \begin{bmatrix} \mathbf{0} \\ \mathbf{L}_{21}^i \end{bmatrix} \quad (113)$$

In \mathbf{L}^i the 3x2 null matrix appears as a submatrix since the two enhanced strains are orthogonal to the three constant stress terms.

In the numerical calculations it was found that both types of enhanced strains lead to the same element stiffness matrices. Since the first type of enhanced strain functions is simpler than the second one we should use the first type. An explicit expression for the first type of enhanced strains is given by

$$\boldsymbol{\varepsilon}^i = \begin{bmatrix} \varepsilon_{xx}^i \\ \varepsilon_{yy}^i \\ \gamma_{xy}^i \end{bmatrix} = \frac{1}{\mathbf{J}(\xi, \eta)} \begin{bmatrix} -\mathbf{b}_2\xi - \mathbf{b}_1\eta & 0 \\ 0 & \mathbf{a}_2\xi + \mathbf{a}_1\eta \\ \mathbf{a}_2\xi + \mathbf{a}_1\eta & -\mathbf{b}_2\xi - \mathbf{b}_1\eta \end{bmatrix} \begin{bmatrix} \lambda_1 \\ \lambda_2 \end{bmatrix} \quad (114)$$

7. Numerical examples

Several linear and nonlinear problems have been chosen in order to test the performance of the proposed four-node element with two enhanced strain modes. The results are compared with analytical solutions and with results obtained from three other elements. Two of these other elements (QM6, P-S) belong to the top performers among the four-node elements. The reference elements are listed in Table 1. All elements we compare are implemented in the nonlinear finite element program FEAP (e.g. see Chap. 16 of [18] and Chap. 15 of [27]).

For the patch test a rectangular domain with five quadrilateral elements was used as suggested by MacNeal/Harder [31]. The proposed element (QE2) passes the test.

Table 1: Elements used for the test examples. (Four node elements with eight degrees of freedom)

| element | element characteristics | reference |
|---------|---|-----------------------------|
| Q4 | bilinear isoparametric displacement element | [28] (see e.g. [29,30]) |
| QM6 | enhanced strain, 4 enhanced strain terms | Taylor/Beresford/Wilson [2] |
| P-S | hybrid stress, 5 stress terms in natural coordinates | Pian/Sumihara [7] |
| QE2 | mixed element, 7 strain/stress terms 2 enhanced strain terms | present paper |

7.1 Beam bending

A beam modeled with five elements is subjected to two load cases (Figure 2). Plane stress conditions are assumed in the model. The results of four different elements for the maximum displacement at point A and the normal stress σ_{xx} at point B are given in Table 2. The stress at point B was calculated as the mean value of the two neighboring nodal stress values. Nodal stresses are obtained in this example by evaluating functions at the nodal coordinates and averaging values from adjacent elements. The proposed element (QE2) shows a very good behavior in this test.

Table 2: Comparison of plane stress solutions obtained with four node elements for cantilever beam problems.

| element | Case 1 | | Case 2 | |
|---------|--------|----------------|--------|----------------|
| | v_A | σ_{xxB} | v_A | σ_{xxB} |
| Q4 | 45.49 | -1604 | 50.80 | -2146 |
| QM6 | 96.07 | -2497 | 97.98 | -3235 |
| P-S | 96.18 | -3001 | 98.05 | -3899 |
| QE2 | 96.5 | -3004 | 98.26 | -3906 |
| exact | 100 | -3000 | 102.6 | -4050 |

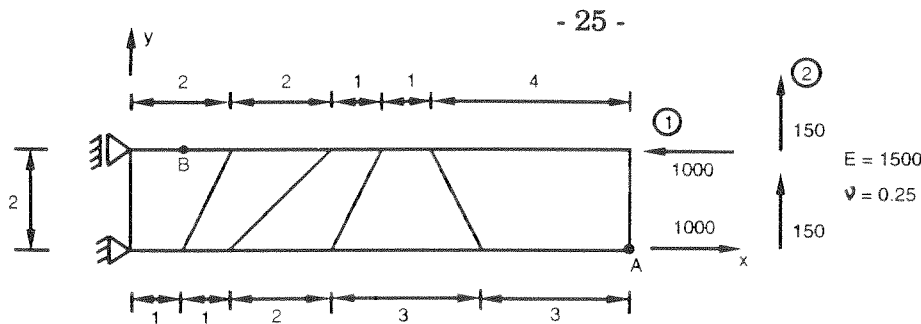


Figure 2: Finite element mesh for cantilever beam problem

7.2 Mesh distortion test for beam bending

In this test a beam under bending is analyzed with only two plane stress elements (Figure 3). The degree of distortion of the element is measured with the distortion parameter Δ . The material parameters are $E = 1500$ and $\nu = 0.25$. From Table 3 we can see that the element QE2 shows the least sensitivity to mesh distortion even for very severe distortions.

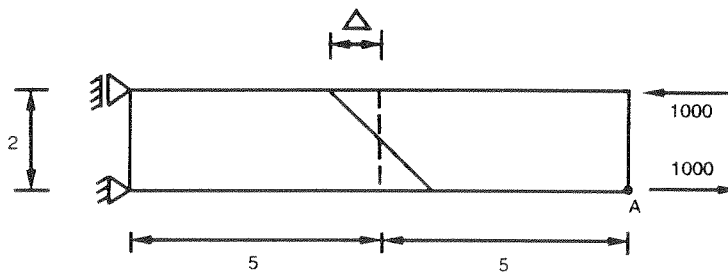


Figure 3: Cantilever beam for the mesh distortion test

Table 3: Displacement v_A of cantilever beam (Figure 3) for different values of the mesh distortion parameter Δ

| displacement v_A | | | | | |
|--------------------|------|-------|-------|-------|-------|
| Δ | Q4 | QM6 | P-S | QE2 | Exact |
| 0 | 28.0 | 100.0 | 100.0 | 100.0 | 100 |
| 0.5 | 21.0 | 80.9 | 81.0 | 84.1 | 100 |
| 1 | 14.1 | 62.7 | 62.9 | 63.4 | 100 |
| 2 | 9.7 | 54.4 | 55.0 | 56.5 | 100 |
| 3 | 8.3 | 53.6 | 54.7 | 57.5 | 100 |
| 4 | 7.2 | 51.2 | 53.1 | 57.9 | 100 |
| 4.9 | 6.2 | 46.8 | 49.8 | 56.9 | 100 |

7.3 Cook's membrane problem

The plane stress structure shown in Figure 4 was suggested by Cook [32] as a test for membrane elements in skewed meshes. The material parameters are $E = 1$ and $\nu = 1/3$. The shear load is distributed uniformly along the right edge. The convergence of the proposed element (QE2) in the energy norm is slightly better than the convergence of the elements QM6 and P-S.

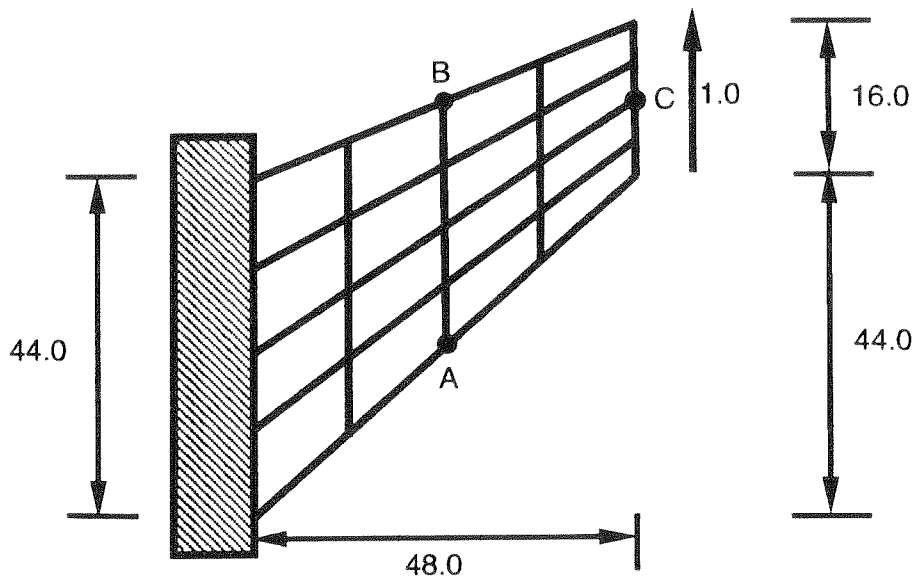


Figure 4: Cook's membrane problem: plane stress structure with unit load uniformly distributed along right edge ($E = 1$, $\nu = 1/3$).

Table 4: Results for the problem shown in Figure 4.

| displacement v at C | | | |
|---------------------|-------|-------|-------|
| element | N=2 | N=4 | N=16 |
| Q4 | 11.85 | 18.30 | 23.43 |
| QM6 | 21.05 | 23.02 | 23.88 |
| P-S | 21.13 | 23.02 | 23.88 |
| QE2 | 21.35 | 23.04 | 23.88 |

| maximum stress at A | | | |
|---------------------|--------|--------|--------|
| element | N=2 | N=4 | N=16 |
| Q4 | 0.1078 | 0.1814 | 0.2353 |
| QM6 | 0.1773 | 0.2225 | 0.2364 |
| P-S | 0.1854 | 0.2241 | 0.2364 |
| QE2 | 0.1956 | 0.2261 | 0.2364 |

| minimum stress at B | | | |
|---------------------|---------|---------|---------|
| element | N=2 | N=4 | N=16 |
| Q4 | -0.0763 | -0.1429 | -0.1995 |
| QM6 | -0.1666 | -0.1854 | -0.2025 |
| P-S | -0.1550 | -0.1856 | -0.2025 |
| QE2 | -0.1448 | -0.1859 | -0.2025 |

| energy | | | |
|---------|-------|-------|-------|
| element | N=2 | N=4 | N=16 |
| Q4 | 11.80 | 18.27 | 23.46 |
| QM6 | 20.92 | 23.02 | 23.93 |
| P-S | 21.00 | 23.02 | 23.93 |
| QE2 | 21.22 | 23.04 | 23.93 |

7.4 Thick-walled cylinder

In order to test the performance of the proposed element for the nearly incompressible case, the thick-walled cylinder problem suggested by MacNeal/Harder [31] was used. The mesh for the plane strain model is given in Figure 5. The material properties are $E = 1$ and $\nu = 0.49/0.499/0.4999/0.49999$.

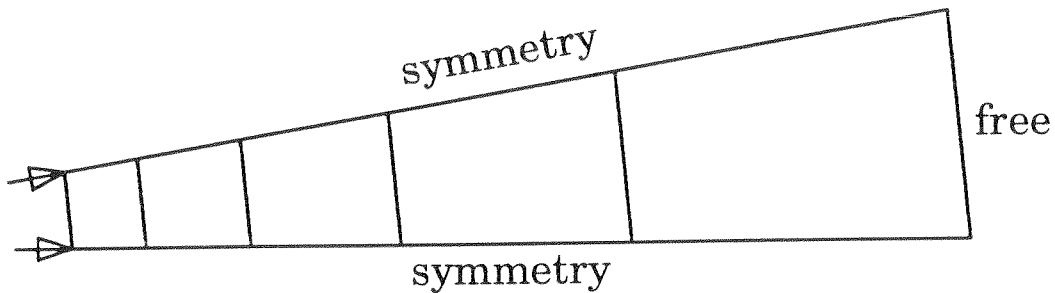


Figure 5: Finite element mesh for thick-walled cylinder. Inner radius = 3.0, outer radius = 9.0, thickness = 1.0, loading: unit pressure at inner radius.

Table 6: Radial displacement at $r = 3$

| ν | Q4 ($\times 10^{-3}$) | QM6, P-S, QE2 ($\times 10^{-3}$) | exact ($\times 10^{-3}$) |
|---------|----------------------------|---------------------------------------|-------------------------------|
| 0.49 | 4.2788 | 4.9959 | 5.0399 |
| 0.499 | 1.8246 | 5.0146 | 5.0602 |
| 0.4999 | 0.2703 | 5.0165 | 5.0623 |
| 0.49999 | 0.0284 | 5.0167 | 5.0625 |

In this test, the isoparametric element Q4 locks for the nearly incompressible case while the other elements give the same satisfactory results (Table 6).

7.5 Elasto-plastic analysis of a tension strip

One quarter of a tension strip with a circular hole is analyzed using the finite element mesh shown in Figure 6. The material properties are specified as

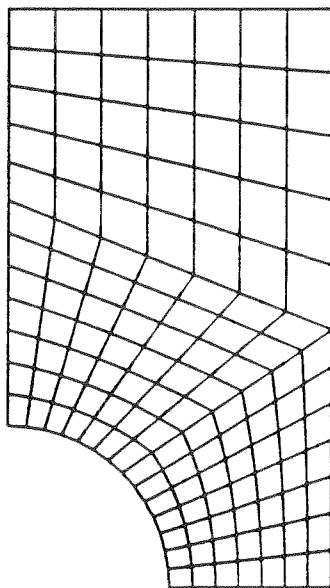
$$E = 7000$$

$$\nu = 0.2$$

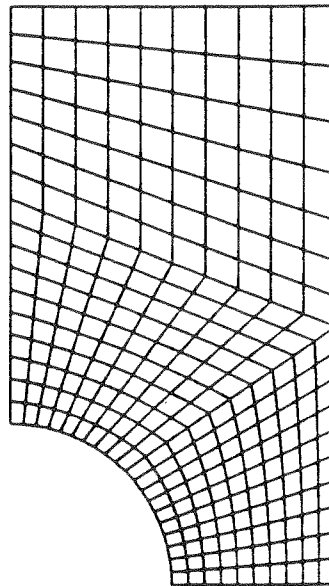
$$\sigma_y^0 = 24.3$$

$$H_{\text{iso}} = H_{\text{kin}} = 0$$

and the J_2 - flow assumption is used. The loading of the tension strip is applied by prescribing the displacements at the top of the meshes in Figure 6. For cyclic loading the load-displacement curve obtained with element QE2 for mesh 2 is shown in Figure 7. In Table 7 the energy convergence rate of the elements QM6 and QE2 are compared. It was observed in the example that the proposed element is able to provide convergence in the Newton algorithm with less or equal iterations the QM6 element requires to converge.



mesh 1



mesh 2

Figure 6: Finite element meshes for tension strip

Table 7: Global Newton iteration energy convergence for elements QM6 and QE2 (mesh 1).

| iteration | load step | | | | | |
|-----------|--------------------|-----------|--------------------|-----------|--------------------|-----------|
| | 2 | | 3 | | 5 | |
| | $(\bar{u} = 0.04)$ | | $(\bar{u} = 0.05)$ | | $(\bar{u} = 0.07)$ | |
| | QM6 | QE2 | QM6 | QE2 | QM6 | QE2 |
| 1 | 4.703e+00 | 4.702e+00 | 4.734e+00 | 4.734e+00 | 4.928e+00 | 4.923e+00 |
| 2 | 4.208e-03 | 4.400e-03 | 6.547e-03 | 6.038e-03 | 5.075e-03 | 3.248e-03 |
| 3 | 9.757e-05 | 5.242e-05 | 1.225e-04 | 4.312e-05 | 6.439e-04 | 1.923e-05 |
| 4 | 6.304e-08 | 1.224e-08 | 6.384e-07 | 4.143e-09 | 1.307e-04 | 8.676e-11 |
| 5 | 1.858e-14 | 2.495e-16 | 5.072e-13 | 3.069e-17 | 2.309e-07 | 1.158e-19 |
| 6 | 5.595e-27 | | 8.283e-24 | | 4.600e-12 | |
| 7 | | | | | 2.613e-21 | |

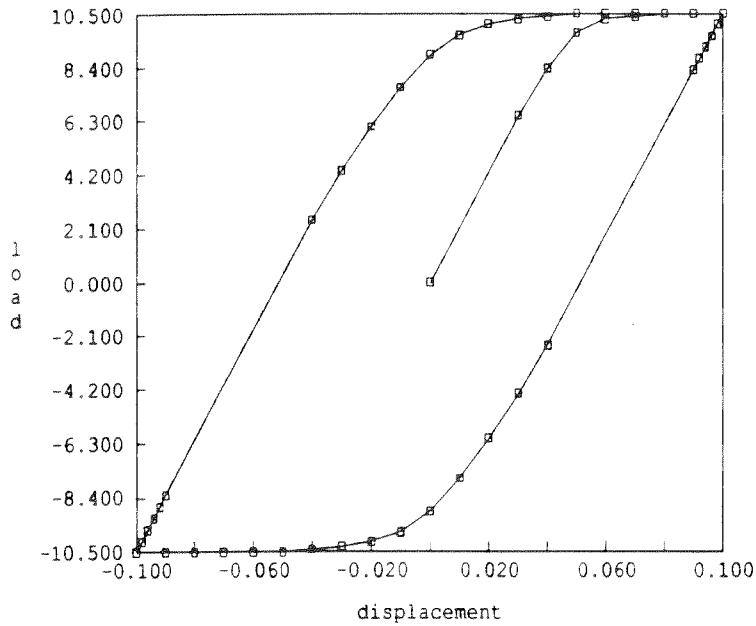


Figure 7: Load displacement curve for the top edge of a tension strip with a circular hole under cyclic loading (element QE2, mesh 2).

7.6 Elasto-plastic analysis of a thick-walled cylinder

The elasto-plastic response of a thick-walled cylinder with inner radius $r_i = 100$ and outer radius $r_o = 200$ is analyzed using the finite element mesh shown in Figure 8. The material parameters in the J_2 -model are chosen as

$$E = 21000$$

$$\nu = 0.3$$

$$\sigma_y^0 = 24.0$$

$$H_{\text{iso}} = H_{\text{kin}} = 0$$

The displacement in radial direction at the inner surface $r = r_i$ is increased and the associated pressure is computed from the resulting finite element nodal reactions. The load-displacement curve obtained with element QE2 is shown in Figure 9. The limit load obtained with element QE2 is 19.18 whereas element QM6 gives the value 19.17.

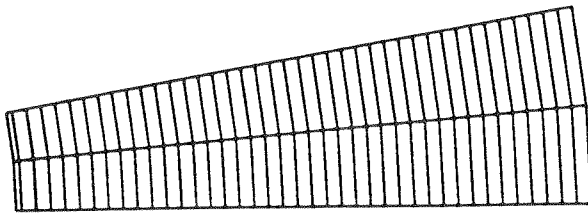


Figure 8: Finite element mesh for thick-walled cylinder

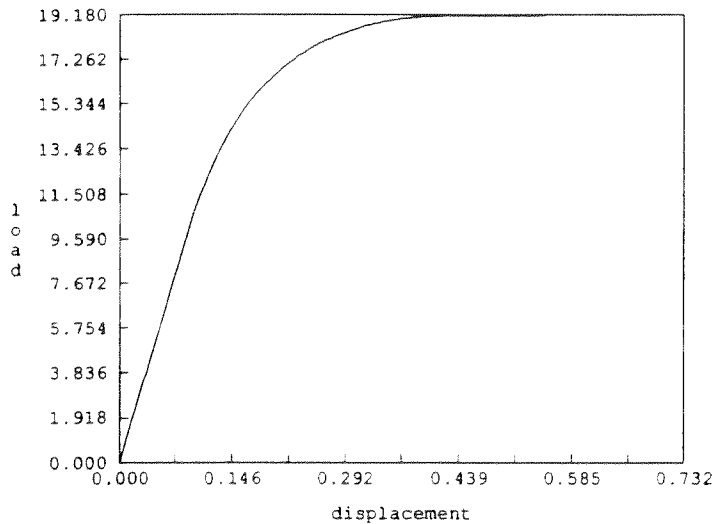


Figure 9: Load-displacement curve for the inner surface of a thick cylinder (element QE2).

The stress distribution for σ_θ in radial direction is shown in Figure 10 for the loading pressures $p = 8$, $p = 14$ and $p = 18$.

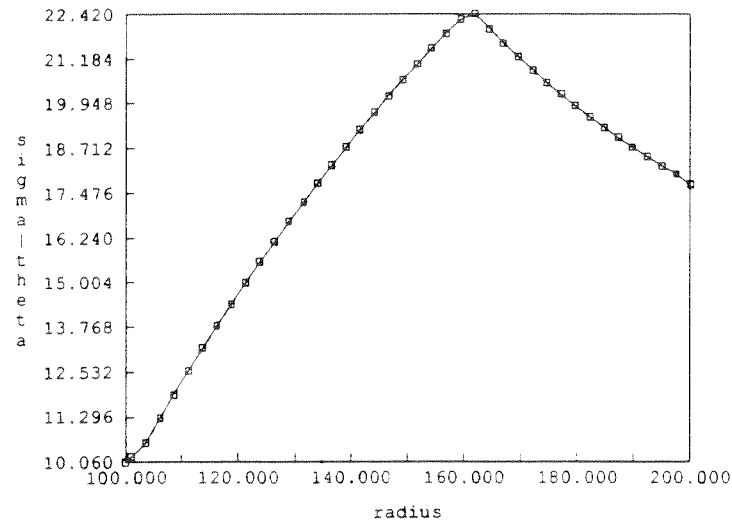
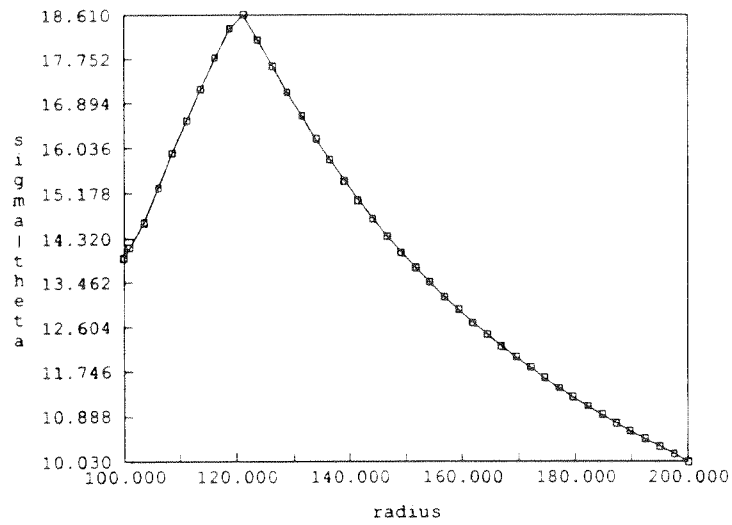
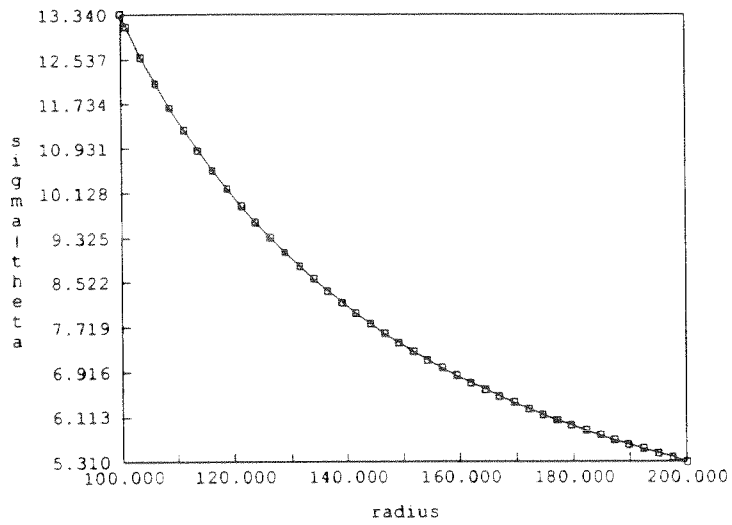


Figure 10: Stress distribution for σ_θ at various pressure values ($p = 8$, $p = 14$ and $p = 18$) for the thick-walled cylinder problem.

For the elasto-plastic analysis the nodal stresses are obtained from the computed values at the Gauss-points of each element by using a bilinear extrapolation to the nodes (see equation (A.1) in the appendix).

8. Concluding remarks

Using a modified Hu-Washizu variational formulation which includes an enhanced strain field, a well performing quadrilateral finite element was derived. It is shown that the modified Hu-Washizu formulation offers an alternative form to derive enhanced strain elements. The main differences between the version of enhanced strains discussed in this paper to the version presented by Simo and Rifai are the following: i) The type of approximation functions for the strain field is different (polynomials in ξ, η versus rational functions of ξ, η). ii) The number of enhanced strain terms is different. (For the proposed quadrilateral element we need only two enhanced strain modes). iii) Unlike in the formulation of Simo and Rifai the stress fields do not drop out from the modified Hu-Washizu variational formulation considered in this paper.

The strain field used satisfies the compatibility equations whereas the chosen stresses satisfy both the equilibrium equations and the compatibility equations for the linear elastic case. The satisfaction of the differential equations for compatibility and equilibrium leads us automatically to a minimum number of stress and strain terms, which is important in order to avoid the problem that an element behaves too stiff. The derived element shows a very good behavior in the linear and non-linear analysis.

Finally it should be mentioned that the considered modified Hu-Washizu variational formulation in connection with properly chosen enhanced strain terms offers new possibilities for reducing nodal degrees of freedom for the group of so called Hybrid-Trefftz elements [27,33,34].

APPENDIX:

Comparison of two versions of enhanced strain methods

In the following the version of enhanced strains used for the element QE2 (denoted by "Version A" in Table 8) is compared to the version of enhanced strains used for the element QM6. The latter version is denoted by "Version B" in Table 8. Simo and Rifai have shown in [3] that the QM6-element by Taylor/Beresford/Wilson is an enhanced strain element with four enhanced strain modes.

In Box 1 and Box 2 the variational equations of the two enhanced strain versions are summarized. Since we want to point out the common features and the differences of the two versions, it suffices here to look at the equations for the linear elastic case. For a comparison of the two versions the main features (ingredients) of the methods are listed in Table 8.

Box 1: Summary of the basic equations for Version A

| Version A: present paper |
|--|
| $\Pi = \int_{\underline{v}} \left[\frac{1}{2} \boldsymbol{\varepsilon}^T \mathbf{E} \boldsymbol{\varepsilon} - \tilde{\mathbf{u}}^T \bar{\mathbf{f}} \right] dV - \int_{\underline{s}} \tilde{\mathbf{u}}^T \bar{\mathbf{T}} dS - \int_{\underline{v}} \boldsymbol{\sigma}^T (\boldsymbol{\varepsilon} - \mathbf{D}\tilde{\mathbf{u}} - \boldsymbol{\varepsilon}^i) dV$ |
| $\int_{\underline{v}} \delta(\mathbf{D}\tilde{\mathbf{u}})^T \boldsymbol{\sigma} dV = \int_{\underline{v}} \delta\tilde{\mathbf{u}}^T \bar{\mathbf{f}} dV + \int_{\underline{s}} \delta\tilde{\mathbf{u}}^T \bar{\mathbf{T}} dS$ |
| $\int_{\underline{v}} \delta\boldsymbol{\varepsilon}^T [\mathbf{E}\boldsymbol{\varepsilon} - \boldsymbol{\sigma}] dV = 0$ |
| $- \int_{\underline{v}} \delta\boldsymbol{\sigma}^T [\boldsymbol{\varepsilon} - \mathbf{D}\tilde{\mathbf{u}} - \boldsymbol{\varepsilon}^i] dV = 0$ |
| $\int_{\underline{v}} (\delta\boldsymbol{\varepsilon}^i)^T \boldsymbol{\sigma} dV = 0$ |

Box 2: Summary of the basic equations for Version B

| Version B: Simo/Rifai [3] |
|--|
| $\Pi = \int_{\mathbb{V}} \left[\frac{1}{2} \boldsymbol{\varepsilon}^T \mathbf{E} \boldsymbol{\varepsilon} - \tilde{\mathbf{u}}^T \bar{\mathbf{f}} \right] dV - \int_{\mathbb{S}} \tilde{\mathbf{u}}^T \bar{\mathbf{T}} dS - \int_{\mathbb{V}} \boldsymbol{\sigma}^T \boldsymbol{\varepsilon}^i dV$ <p>where $\boldsymbol{\varepsilon} = \mathbf{D}\tilde{\mathbf{u}} + \boldsymbol{\varepsilon}^i$</p> $\int_{\mathbb{V}} \delta(\mathbf{D}\tilde{\mathbf{u}})^T \left[\mathbf{E}(\mathbf{D}\tilde{\mathbf{u}} + \boldsymbol{\varepsilon}^i) \right] dV = \int_{\mathbb{V}} \delta \tilde{\mathbf{u}}^T \bar{\mathbf{f}} dV + \int_{\mathbb{S}} \delta \tilde{\mathbf{u}}^T \bar{\mathbf{T}} dS$ $\int_{\mathbb{V}} (\delta \boldsymbol{\varepsilon}^i)^T \left[\mathbf{E}(\mathbf{D}\tilde{\mathbf{u}} + \boldsymbol{\varepsilon}^i) - \boldsymbol{\sigma} \right] dV = 0$ $\int_{\mathbb{V}} \delta \boldsymbol{\sigma}^T \boldsymbol{\varepsilon}^i dV = 0$ |

The common feature of both versions is that the enhanced strains are constructed such that they are orthogonal to a set of linearly independent stress functions. Since there are different types of stresses in the two formulations we want to distinguish them through the following notation:

assumed stresses: $\boldsymbol{\sigma}$

reference stresses: $\boldsymbol{\sigma}^*$

output stresses: $\hat{\boldsymbol{\sigma}}$

output stresses projected from Gauss-points: $\hat{\boldsymbol{\sigma}}_p$

The output stresses for the nodes can be obtained by

- a) evaluating the assumed strains at the element nodes and using the constitutive equations
- b) evaluating assumed stresses at the element nodes
- c) projecting the discrete stress values at the Gauss-points to the nodes with the aid of a bilinear extrapolation function.

In the case of stress projection we denote the stress values at the four Gauss-points with $\hat{\boldsymbol{\sigma}}_i^*$ ($i=1,4$) and obtain the stresses at the nodes by substituting the nodal coordinates ($\xi = \xi_i, \eta = \eta_i$) into

$$\hat{\boldsymbol{\sigma}}_p = \frac{1}{4} \left[(1 - \sqrt{3}\xi)(1 - \sqrt{3}\eta)\hat{\boldsymbol{\sigma}}_1^* + (1 + \sqrt{3}\xi)(1 - \sqrt{3}\eta)\hat{\boldsymbol{\sigma}}_2^* \right. \\ \left. + (1 + \sqrt{3}\xi)(1 + \sqrt{3}\eta)\hat{\boldsymbol{\sigma}}_3^* + (1 - \sqrt{3}\xi)(1 + \sqrt{3}\eta)\hat{\boldsymbol{\sigma}}_4^* \right] \quad (\text{A.1})$$

Table 8: Comparison of two versions for enhanced strain methods

| | Version A | Version B |
|---|---|---|
| assumed stresses | $\boldsymbol{\sigma} = \mathbf{P}\boldsymbol{\beta}$ equilibrium equations are satisfied a priori; stress parameters $\boldsymbol{\beta}$ can be computed from variational formulation | $\boldsymbol{\sigma} = \boldsymbol{\sigma}^*$ equilibrium equations are not satisfied a priori; stress parameters $\boldsymbol{\beta}^*$ cannot be computed from variational formulation |
| reference stresses | $\boldsymbol{\sigma}^* = \mathbf{F}_0\mathbf{P}^*(\xi, \eta)\boldsymbol{\beta}^*$ | $\boldsymbol{\sigma}^* = \mathbf{F}_0\mathbf{P}^*(\xi, \eta)\boldsymbol{\beta}^*$ |
| enhanced strain | $\boldsymbol{\varepsilon}^i = \mathbf{B}^i\boldsymbol{\lambda}$ | $\boldsymbol{\varepsilon}^i = \mathbf{B}^i\boldsymbol{\lambda}$ |
| number of enhanced strain terms | 2 | 4 |
| assumed strains | $\boldsymbol{\varepsilon} = \mathbf{A}\boldsymbol{\beta}$ polynomials in ξ, η | $\boldsymbol{\varepsilon} = \tilde{\boldsymbol{\varepsilon}} + \boldsymbol{\varepsilon}^i$ $= \mathbf{B}\mathbf{q} + \mathbf{B}^i\boldsymbol{\lambda}$ rational functions in ξ, η |
| assumed displacements | $\tilde{\mathbf{u}} = \mathbf{N}\mathbf{q}$ | $\tilde{\mathbf{u}} = \mathbf{N}\mathbf{q}$ |
| assumed displacements to get strains $\boldsymbol{\varepsilon} = \mathbf{D}\mathbf{u}$ | $\mathbf{u} = \mathbf{U}\boldsymbol{\beta}$ | not needed |
| output stresses | $\hat{\boldsymbol{\sigma}} = \boldsymbol{\sigma}$ $= \mathbf{E}\boldsymbol{\varepsilon}$ | $\hat{\boldsymbol{\sigma}} = \mathbf{E}(\mathbf{B}\mathbf{q} + \mathbf{B}^i\boldsymbol{\lambda})$ $= \mathbf{E}\boldsymbol{\varepsilon}$ |
| output stresses projected from Gauss-points | $\hat{\boldsymbol{\sigma}}_p = \hat{\boldsymbol{\sigma}} = \boldsymbol{\sigma}$ at nodes and at Gauss-points | $\hat{\boldsymbol{\sigma}}_p \neq \hat{\boldsymbol{\sigma}}$ at nodes $\hat{\boldsymbol{\sigma}}_p = \hat{\boldsymbol{\sigma}}$ at Gauss-points |
| | $\int_{\mathbb{V}} \delta \boldsymbol{\sigma}^{*\mathbf{T}} \boldsymbol{\varepsilon}^i dV = \int_{\mathbb{V}} \delta \boldsymbol{\varepsilon}^{i\mathbf{T}} \boldsymbol{\sigma}^* dV = 0$ satisfied a priori | $\int_{\mathbb{V}} \delta \boldsymbol{\sigma}^{*\mathbf{T}} \boldsymbol{\varepsilon}^i dV = \int_{\mathbb{V}} \delta \boldsymbol{\varepsilon}^{i\mathbf{T}} \boldsymbol{\sigma}^* dV = 0$ satisfied a priori |
| | $\int_{\mathbb{V}} \delta \boldsymbol{\sigma}^{\mathbf{T}} \boldsymbol{\varepsilon}^i dV \neq 0$ | $\int_{\mathbb{V}} \delta \hat{\boldsymbol{\sigma}}^{\mathbf{T}} \boldsymbol{\varepsilon}^i dV \neq 0$ |
| | $\int_{\mathbb{V}} \delta \boldsymbol{\varepsilon}^{i\mathbf{T}} \boldsymbol{\sigma} dV = 0$ gives constraint equations for $\boldsymbol{\beta}$ | $\int_{\mathbb{V}} \delta \boldsymbol{\varepsilon}^{i\mathbf{T}} \hat{\boldsymbol{\sigma}} dV = 0$ gives constraint equations for \mathbf{q} and $\boldsymbol{\lambda}$ |

In version B, the parameters of the assumed stresses can not be computed from the variational formulation because the associated coefficient matrix is a null matrix due to the orthogonality requirement that enhanced strains do not work on the assumed stresses.

In version B the assumed stresses are not the same as the output stresses, and we can consider (identify) the assumed stresses σ in this case as reference stresses σ^* which are used to construct enhanced strain terms such that the condition (15) is satisfied. The output stresses $\hat{\sigma}$ in version B are obtained from the assumed strains ε by using the constitutive equations.

For version A we can obtain admissible enhanced strain functions by using the same reference stresses σ^* for the orthogonality condition as in version B. The number of enhanced strain terms used in the two versions is different. The reference stresses σ^* in version A are different from the assumed stresses σ . In version A we are able to compute the stress parameters of the assumed stresses from the variational formulation so that for the linear elastic case the output stresses will be equal to the assumed stresses. The common feature of both versions is that the enhanced strains are orthogonal to the reference stresses σ^* but they are not orthogonal to the output stresses.

In both methods the requirement

$$\int_V \delta \varepsilon^i \hat{\sigma}^T dV = 0 \quad (\text{A.2})$$

leads to constraint equations (i.e. for β in version A, and for \mathbf{q} , λ in version B).

The strains in version A are polynomials in ξ , η whereas the strain field ε for version B contains rational functions in ξ , η for a general quadrilateral element domain.

A particular feature of the assumed stresses σ in version A is that they satisfy the equilibrium equations a priori.

For the considered element the reference stresses σ^* are given in equation (105) whereas the assumed stresses σ are given with equation (90).

REFERENCES

- [1] E.L. Wilson, R.L. Taylor, W.P.Doherty and J. Ghaboussi, "Incompatible displacement models", in: Numerical and Computer Methods in Structural Mechanics (Ed. S.J. Fenves, et al.) Academic Press, New York, 1973, p.43

- [2] R.L. Taylor, P.J. Beresford and E.L. Wilson, "A non-conforming element for stress analysis", *Int. J. Numer. Meth. Eng.*, 10, 1211 - 1219, (1976).
- [3] J.C. Simo and M.S. Rifai, "A class of mixed assumed strain methods and the method of incompatible modes", *Int. J. Numer. Meth. Eng.*, 29, 1595 - 1638, (1990).
- [4] C.-C. Wu, M.-G. Huang and T.H.H. Pian, "Consistency condition and convergence criteria of incompatible elements: General formulation of incompatible functions and its application", *Computers & Structures* 27, 639 - 644, (1987).
- [5] T.J.R. Hughes, "Equivalence of finite elements for nearly incompressible elasticity", *J. Appl. Mech.* 44, 181 - 183, (1977).
- [6] T.J.R. Hughes, "Generalizing of selective integration procedures to anisotropic and nonlinear media", *Int. J. Numer. Meth. Eng.*, 15, 1413 - 1418, (1980).
- [7] T.H.H. Pian and K. Sumihara, "Rational approach for assumed stress elements", *Int. J. Numer. Meth. Eng.*, 20, 1685 - 1695, (1984).
- [8] T.H.H. Pian, "Derivation of element stiffness matrices by assumed stress distributions", *AIAA Journal*, 2, 1333 - 1336, (1964).
- [9] R.L. Spilker, S.M. Maskeri and E. Kania, "Plane isoparametric hybrid-stress elements: invariance and optimal sampling", *Int. J. Numer. Meth. Eng.*, 17, 1469 - 1496, (1981).
- [10] T.H.H. Pian and P. Tong, "Relations between incompatible displacement model and hybrid stress model", *Int. J. Numer. Meth. Eng.*, 22, 173 - 181, (1986).
- [11] T.H.H. Pian and C.C. Wu, "A rational approach for assuming stress terms for hybrid finite element formulations", *Int. J. Numer. Meth. Eng.*, 26, 2331 - 2343, (1988).
- [12] M. Ortiz and E.P. Popov, "Accuracy and stability of integration algorithms for elasto-plastic constitutive relations", *Int. J. Numer. Meth. Eng.*, 21, 1561 - 1576, (1985).
- [13] J.C. Simo and R.L. Taylor, "Consistent tangent operators for rate-independent elasto-plasticity", *Comput. Methods Appl. Mech. Engrg.* 48, 101 - 118, (1985).
- [14] J.C. Simo, J.G. Kennedy and R.L. Taylor, "Complementary mixed finite element formulations for elasto-plasticity", *Comput. Methods Appl. Mech. Engrg.* 74, 177 - 206, (1989).
- [15] J.C. Simo and R.L. Taylor, "A return mapping algorithm for plane stress elasto-plasticity", *Int. J. Numer. Meth. Eng.*, 22, 649 - 670, (1986).
- [16] D.R.J. Owen and E. Hinton, "Finite elements in Plasticity: Theory and Practice", Pineridge Press, Swansea, 1980.
- [17] W.F. Chen and D.J. Han, "Plasticity for Structural Engineers", Springer-Verlag, New York, Berlin, 1988.
- [18] O.C. Zienkiewicz, and R.L. Taylor, "The Finite Element Method", Volume 2: Solid and Fluid Mechanics, Dynamics and Non-Linearity, McGraw-Hill, London, New York, 1991
- [19] R. Piltner, "The derivation of a thick and thin plate formulation without ad hoc assumptions", *Journal of Elasticity*, 29, 133 - 173 (1992)
- [20] R. Piltner, "On the representation of three-dimensional elasticity solutions with the aid of complex valued functions", *Journal of Elasticity*, 22, 45 - 55 (1989)

- [21] R. Piltner, "The representation of three-dimensional elastic displacement fields with the aid of complex valued functions for several curvilinear coordinates", *Mechanics Research Communications*, 15 (2), 79 - 85 (1988)
- [22] R. Piltner, "The application of a complex 3-dimensional elasticity solution representation for the analysis of a thick rectangular plate", *Acta Mechanica*, 75, 77 - 91, (1988).
- [23] R. Piltner, "The use of complex valued functions for the solution of three-dimensional elasticity problems", *Journal of Elasticity*, 18, 191 - 225 (1987)
- [24] Muskhelishvili, N.I. *Some Basic Problems of the Mathematical Theory of Elasticity*, Noordhoff, Groningen, Holland , 1953.
- [25] R.L. Taylor, O.C. Zienkiewicz, J.C. Simo and A.H.C. Chan, "The patch test for mixed formulations", *Int. J. Numer. Meth. Eng.*, 22, 32 - 62, (1986).
- [26] S.L. Weissman and R.L. Taylor, "A unified approach to mixed finite element methods: Application to in-plane problems", *Comput. Methods Appl. Mech. Engrg.* 98, 127 - 151, (1992).
- [27] O.C. Zienkiewicz, and R.L. Taylor, "The Finite Element Method", Volume 1: Basic Formulations and Linear Problems, McGraw-Hill, London, New York, 1989
- [28] I.C. Taig, "Structural analysis by the matrix displacement method", *English Electric Aviation Report No. S017*, 1961.
- [29] T.J.R. Hughes, "The Finite Element Method", Prentice-Hall, Englewood Cliffs, N.J., 1987.
- [30] K.-J. Bathe, E.L. Wilson, "Numerical Methods in Finite Element Analysis", Prentice-Hall, Englewood Cliffs, New Jersey, 1976.
- [31] R.H. MacNeal and R.L. Harder, "A proposed standard set of problems to test finite element accuracy", *Finite Elements Anal. Design* 1, 2 - 20, (1985).
- [32] R.D. Cook, "A plane hybrid element with rotational d.o.f. and adjustable stiffness", *Int. J. Numer. Meth. Eng.*, 24, 1499 - 1508, (1987).
- [33] J. Jirousek, and L. Guex, "The hybrid-Trefftz finite element model and its application to plate bending", *Int. J. Numer. Methods Eng.*, 23, 651 - 693, (1986).
- [34] R. Piltner, "A quadrilateral hybrid-Trefftz plate bending element for the inclusion of warping based on a three-dimensional plate formulation", *Int. J. Num. Methods Eng.*, 33, 387 - 408 (1992)